IN-CORE POWER PREDICTION OF THE NIGERIA RESEARCH REACTOR-I (NIRR-1) USING DOSE-RATE AND TEMPERATURE MEASUREMENTS

BY

YAHAYA JIBRIN

DEPARTMENT OF PHYSICS,
FACULTY OF SCIENCE,
AHMADU BELLO UNIVERSITY,
ZARIA, NIGERIA

MAY, 2016

IN-CORE POWER PREDICTION OF THE NIGERIA RESEARCH REACTOR-I (NIRR-1) USING DOSE-RATE AND TEMPERATURE MEASUREMENTS

BY

YAHAYA JIBRIN
(MSC/SCI/37382/2012-2013)

A THESIS SUBMITTED TO THE SCHOOL OF POST GRADUATE STUDIES,
AHMADU BELLO UNIVERSITY, ZARIA

IN PARTIAL FULFILLMENT OF THE REQUIREMENTS FOR THE AWARD OF
MASTER OF SCIENCE DEGREE IN NUCLEAR PHYSICS

DEPARTMENT OF PHYSICS,
FACULTY OF SCIENCE,
AHMADU BELLO UNIVERSITY,
ZARIA, NIGERIA

MAY, 2016

DECLARATION

I declare that the work presented in this thesis entitled **"IN-CORE POWER PREDICTION OF THE NIGERIA RESEARCH REACTOR-I (NIRR-1) USING DOSE-RATE AND TEMPERATURE MEASUREMENTS"** has been carried out by me in the Department of Physics, and supervised by Dr. Y.V Ibrahim and Dr. U. Sadiq. To the best of my knowledge, no part of this thesis was previously presented for another degree or diploma at this or any other Institution. Where other peoples work has been quoted, it is duly acknowledge and referenced.

Yahaya Jibrin _____ _____

(Name) (Signature) (Date**)**

CERTIFICATION

This thesis entitled **"IN-CORE POWER PREDICTION OF THE NIGERIA RESEARCH REACTOR-I (NIRR-1) USING DOSE-RATE AND TEMPERATURE MEASUREMENTS"** by Yahaya Jibrin meets the regulations governing the award of the degree of Masters of Science (Nuclear Physics) of the Ahmadu Bello University, and is approved for its contribution to knowledge and literary presentation.

Dr. Y.V IBRAHIM		
Chairman, Supervisory Committee (Name)	(Signature)	(Date)
Dr. UMAR SADIQ		
Member, Supervisory Committee (Name)	(Signature)	(Date)
Dr. UMAR SADIQ		
Head of Department (Name)	(Signature)	(Date)
Prof. K. BALA		
Dean, School of Postgraduate Studies (Name)	(Signature)	(Date)

DEDICATION

I affectionally dedicate this research work to the memory of my beloved late mother HAJIYA FATIMA JIBRIN. May ALLAH forgive and reward her with AL-JANNATIL FIRDAUS.

ACKNOWLEDGEMENT

First and foremost I would like to thank ALLAH the Almighty for his protection, guidance and making this work a reality.

I would like to express my profound gratitude and indebtedness to my main supervisor Dr. Y.V Ibrahim for his understanding, co-operation, advice and encouragement towards the successful execution of this project and Dr. U. Sadiq (Head of Department), for providing the enabling environment for the completion of my programme, counting me among his own and for his moral support, Sir I am grateful to God for bringing you in to my life. Also thanks the entire staff of Physics Department, Ahmadu Bello University Zaria.

I cannot forget the contribution of my brother Dr. Jibrin Jibrin of the Department of Chemical Pathology, Ahmadu Bello University Teaching Hospital Shika, Zaria. My profound and sincere thanks goes to him, for his moral and financial support throughout my studies. Also, the support of his family Hajiya Salamatu and Mallama Munirah is highly appreciated.

My profound gratitude goes to the entire staff of Centre for Energy Research and Training (CERT) Ahmadu Bello University Zaria, my friends and colleagues: Iliyasu, Sunday, Babangida, my entire classmate and all other well-wishers. I say thank you all. May Almighty ALLAH reward you all abundantly (Amin).

ABSTRACT

This study presents the result of the in-core power prediction of the Nigeria Research Reactor-1 (NIRR-1) using dose-rate, neutron flux and temperature measurements, a low power Miniature Neutron Source Reactor (MNSR). In this work, measurements of the dose rate, neutron flux, inlet temperature and outlet temperature were made for three different power levels (6.2 kW, 15.5 kW and 31 kW) at three stages: The first was immediately after the reactor start-up (0 minute). The second one was at 105 minutes elapsed time of the reactor operation. The final one was made at every one hour for five hours of reactor operation at half power (maximum neutron flux of 5×10^{11} n/cm²-s). The data obtained from the measurements were used to monitor the in-core reactor power. The values of the dose-rate obtained at 0 minute (at 6.2 kW, 15.5 kW and 31 kW power levels) are 6.1 $\mu Sv/hr$, 15.0 $\mu Sv/hr$ and 34.2 $\mu Sv/hr$ respectively and the corresponding predicted power at this time were 6.8 kW, 15.4 kW and 33.8 kW respectively. The values of the dose-rate obtained at 105 minutes (at 6.2 kW, 15.5 kW and 31 kW power levels) are 7.8 $\mu Sv/hr$, 21.5 $\mu Sv/hr$ and 37.4 $\mu Sv/hr$ respectively and the corresponding predicted power were 6.3 kW, 17.8 kW and 31.1 kW respectively. For temperature measurement (7.8 °C, 12.7 °C and 18.7 °C) and (7.2 °C, 12.4 °C and 18.3 °C) at 0 minute and 105 minutes, the results obtained were: (6.9 kW, 14.8 kW and 28.0 kW) and (6.4 kW, 15.4 kW and 29.0 kW) respectively. Furthermore, for the measured thermal neutron flux ($2.07\text{x}10^{11}$ n/cm^2-s, $5.53\text{x}10^{11}$ n/cm^2-s and $1.13\text{x}10^{12}$ n/cm^2-s) and ($2.06\text{x}10^{11}$ n/cm^2-s, $5.70\text{x}10^{11}$n/cm^2-s and $1.16\text{x}10^{12}$ n/cm^2-s) at 0 minute and 105 minutes, the results obtained were: (6.21 kW, 16.60 kW and 33.90 kW) and (6.18 kW, 17.10 kW and 34.80 kW) respectively. The result obtained at full power (31 kW) in this work compare well with 29.5kW calculated from fitting formula based on the stimulation test data during initial startup as reported in the Nigeria Research Reactor -1 Safety

Analysis Report (2005). The results obtained also compare well with the rated thermal power by the manufacturer. In the final stage, the steady state operation of NIRR-1 was investigated at half power. Real steady state was achieved after four hours of reactor operation.

TABLE OF CONTENTS

Content **Page**

CHAPTER FIVE: CONCLUSION AND RECOMMENDATION

LIST OF TABLES

LIST OF FIGURES

LIST OF ABBREVIATION AND ACRONYMS

ANOVA	Analysis of Variance
CERT	Centre for Energy Research and Training
CIC	Compensated Ionization Chamber
FC	Fission Chamber
HWZPR	Heavy Water Zero Power Reactor
INSARR	Integrated Safety Assessment for Research Reactor
LWZPR	Low Water Zero Power Reactor
MNSR	Miniature Neutron Source Reactor
NAA	Neutron Activation Analysis
NIRR-1	Nigeria Research Reactore-1
OLCs	Operational Limiting Conditions
RTC	Reactivity Temperature Coefficient
SPSS	Statistical Package for the Social Sciences
UIC	Uncompensated Ionization Chamber

CHAPTER ONE
INTRODUCTION

1.1 GENERAL INTRODUCTION

During reactor operation, numerous parameters such as temperature, pressure, power level and flow are continuously monitored and controlled to ensure safe and stable operation of the reactor. The specific effects of variations in these parameters vary greatly depending upon reactor design. A change in reactor power level is considered as one of the most important physical quantities used to assess the inherent safety of a reactor as it can result in a change in reactivity if the power level change results in a change in system temperature (DOE, 1993). A change in power during reactor operation generally alters the temperatures of the fuel, moderator, and coolant, and a change in temperature of any of these components causes a change in reactivity that, in turn, affects reactor operation (a feedback effect). Temperature variation in a reactor changes the microscopic reaction rate and the density of the moderator and consequently, the infinite multiplication factor. This results in the addition of either positive or negative reactivity (Ott and Bezella, 1989; DOE, 1993).

The most important factor in reactor control is the precise information about reactor power at any moment. Accurate reactor power measurement is required not only for safety purposes but also by research reactor users for doing different experiments. Criteria such as redundancy, diversity, precision, speed, reliability and availability are significant for reactor power measurement. However, for reactor safety, it is extremely important to observe two factors: redundancy and diversity of techniques in power measurement (Lu, 1964; Arakani and Gharib, 2009). Normally reactor power monitoring is done by employing a nuclear neutronic equipment, which is calibrated by thermal and absolute

fission rates. Consequently, reactor power can be monitored at any time in the control room by instruments such as fission chamber, compensation ionization chamber (CIC), uncompensation ionization chamber, gamma self-power, neutron self-power and gamma and neutron thermometers. These instruments must be re-calibrated regularly (Jalali *et al.*, 2013).

Due to safety requirements, more than one safety feature measurement is required in the study of reactor power and flux behavior with respect to changes in core-coolant temperature as shown by previous workers in the field of safety and thermal hydraulic behavior of Miniature Neutron Source Reactor [MNSR] (Hainoun and Alisa, 2005; Jonah *et al.*, 2007).

It is important to understand the principles that determine how a reactor responds during all modes of operation. Special measures must be taken during the startup of a reactor to ensure that expected responses are occurring. During power operation, control of the flux shape is necessary to ensure operation within limits and maximum core performance. Even when a reactor is shut down, the fact that the fission products created by the fission process continue to generate heat results in a need to monitor support systems to ensure adequate cooling of the core (DOE, 1993).

Over the years, various methods such as thermal hydraulic methods, neutron flux measurement, Cherenkov radiation intensity measurement, measurement of delayed neutrons rate, ^{16}N gamma activity and gamma dose-rate (Khamis and Jamal, 2006; Armozd *et al.*, 2011) have been developed worldwide for the determination of the power level in research reactors. However, due to the wide spectrum of research reactors having various power levels and different designs, it is rather cumbersome to select a specific or common method that could be applicable for most of the reactors (IAEA, 1995).

In power reactors, common methods for the determination of power level depend on thermal hydraulic techniques where measurement of flow rates and temperature difference across the core are made (Sturm, 1961). Such method, in general, measures the heat ejected from the core and dissipated either directly through the primary loop or ejected through the secondary system. Once an equilibrium is reached, i.e., temperatures at various locations in the primary and secondary loops become stable, the reactor power is considered stable and constant.

For research reactors, several methods for power calibration have been worked out. In part, they involve the use of thermal expansion of the pool water (Straka, 1984). For example, one method calls for the measurement of the change in height of the pool surface water level resulting from the thermal expansion of the bulk of water in the reactor pool. Another method, the volumetric thermal expansion of water, which relates the amount of heat being transferred into the reactor pool. This method is considered less accurate than the first one. One common method is the use of a calibrated electrical heater in a calorimetric procedure (Whittemore *et al*., 1988), where the rate of the rise of the water temperature of the pool is measured. In this case, the operation of the reactor is continued so as to give the same rate of rise of water temperature. Then, the reactor thermal power is established as the value produced by the electrical heaters. Such a method is considered, in some cases, inconvenient due to the repeated use of the electrical heaters where calibration of the heaters themselves should be made and checked. In addition, complete mixing of the pool water is not assured during such measurements. Modification of the previous method, especially when a need arises for the calibration of the nominal power level of the reactor, was suggested (Whittemore *et al*., 1988). The addition of a stirrer to the pool assures a uniform temperature distribution within the pool.

Other techniques for the determination of the power level in research reactors, where flow rate measurements seem difficult, have also been suggested (Bebbs, 1958; Lamarsh, 1966). The most common methods depend either on the measurement of the absolute thermal neutron flux using calibrated flux monitors (such as gold or dysprosium) inserted in an irradiation site in the core (Parry, 1991), the measurement of released-gases activities either on top of the reactor pool, or measurement of activation products in the primary water of the reactor. In the later method, measurement is made of the discharged of (n,γ) and (n,p) reactions, respectively. Furthermore, a method for the determination of in-core power in low-energy research reactors by the measurement of ^{16}N and ^{18}F in the primary coolant has been reported (Beeley *et al*., 1997).

The Nigeria Research Reactor-1 (NIRR-1) is a 31 kW tank-in-pool Miniature Neutron Source Reactor (MNSR). The small core of the reactor is cooled and moderated by light water while the annular beryllium surrounding the core acts as reflector. The MNSR designer's objective was to achieve a core of low critical mass with a small compact core structure (Yang, 1992). Under-moderation was achieved by choosing highly enriched uranium (90.2%) as fuel material and light water as moderator and coolant (Zhu, 1990). The structure of the reactor was simplified by arranging the irradiation sites in and just after the beryllium reflectors. This has reduced the effect of the control rod movement on the reactivity and flux distribution in all the irradiation sites. Detailed description of NIRR-1 has been reported elsewhere (Ahmed *et al*. 2002; Balogun, 2003; Jonah *et al*., 2006).

At the pool-type Nigeria Research Reactor-1 (NIRR-1), the power is measured by employing fission chambers at a two small vertical holes each 10 mm in diameter and 190 mm deep on the side annular beryllium reflector on the same circle as the inner irradiation

sites to monitor neutron flux at each irradiation site and provide control signal for the reactor automatic control system, evaluation of reactor experiments, accurate determination and calculation of fuel element burn-up and isotopic composition of burned fuel, normalization of calculated neutron fluxes and dose rates (SAR, 2005; Manca, 2011). As mentioned earlier, one of the methods of reactor power determination is the measurement of gamma dose-rate on top of the MNSR surface produced due to the fission reaction inside the reactor core. This work presents the methodology for predicting the in-core power of NIRR-1 by dose-rate and temperature measurements.

1.2 STATEMENT OF RESEARCH PROBLEM

From the time when NIRR-1 was commissioned in 2004 till date, several attempts were made to predict some parameters such as flux variation using thermal hydraulic (Ahmed *et al*., 2008), its maximum operable time using control rod critical depth of insertion (Ahmed *et al*., 2011), and its flux stability using foils activation method (Musa *et al*., 2012). No efforts were made to predict the in-core power using neutron flux, dose-rate and temperature measurements. This work was undertaken in order to analyze the accuracy of the methods and recommend ways to adopt one of the methods for routine estimation of NIRR-1 power.

1.3 RESEARCH AIM AND OBJECTIVES

The aim of this research work is to estimate the in-core power of Nigeria Research Reactor-1 (NIRR-1).

The objectives are to achieve the following:

a. To predict the power level in the NIRR-1 knowing the measured neutron flux, dose-rate on top of the reactor and temperature rise.

b. Comparison between the powers predicted using neutron flux, dose-rate and temperature measurements with the rated thermal power of NIRR-1 by the manufacturer.

c. Adopt a method for the in-core power prediction of NIRR-1.

d. To predict the average core temperature of NIRR-1 from dose-rate and temperature measurements.

e. To investigate NIRR-1 stability.

1.4 JUSTIFICATION

The knowledge of online reactor power level is a problem to many MNSR reactor operators. The most obvious need for an accurate determination of the reactor power level is that of satisfying the safety criteria established for a given system and operational limiting conditions (Bullock, 1965). Research reactors, however, are frequently involved with experiments requiring an accurate measure of the reactor power. Furthermore, the statistical significance of experimental measurements that are normalized to reactor power level cannot be meaningfully stated unless the statistical variation of the reactor power level measurement is known (Bullock, 1965).

Accurate reactor power prediction is important for: safe monitoring and evaluation of reactor operation, as the reactor power signal is used in the reactor automatic control system, evaluation of reactor experiments, accurate determination and calculation of fuel element burn-up and isotopic composition of burned fuel, normalization of calculated neutron fluxes and dose rates (Manca, 2011). Moreover, the Operational Limiting Conditions (OLCs) of NIRR-1 reactor prescribes the power limits of the reactor and thus the recommendation by the Integrated Safety Assessment for Research Reactor (INSARR) mission 2009 supports for the inclusion of power display on the control console. Consequently, the need to measure the in-core power is very crucial and that is the basis for this research work.

The power developed by a reactor is a quantity of great interest for practical reasons. Power is related to the neutron population and to the mass of fissile material present. Measurement of the quantity of heat produced per unit time in a reactor core is essential to the safe control, stability and operation of the reactor as well as the reliability of the research reactor.

1.5 PREVIOUS WORK

Bullock (1965) measured the absolute power of the Ford Nuclear Reactor. The method used was calorimetric in which the pool water system is treated as a calorimeter and measurements were made to determine the rate at which energy is being added to the system. The results show that the calorimetric power determination technique can be used to determine the reactor power level for systems having low heat losses, to within a few percent. The method can be used to calibrate relative power measuring devices and to determine the confidence level for reference power meters. However, such a method is

considered, in some cases, inconvenient due to the repeated use of the electrical heaters where calibration of the heaters themselves should be made and checked. In addition, complete mixing of the pool water is not assured during such measurements (Khamis and Jamal, 2006).

The prediction of the in-core power and the average core temperature of the Syrian Miniature Neutron Source Reactor was investigated by Khamis and Jamal (2006). The method used in the measurements was a dose-rate on the top surface of the Miniature Neuron Source Reactor. The results show that an experimental correlation for the prediction of both reactor power level and average core-coolant temperature as a functions of dose-rate measurement seems to agree closely with the real data.

Recently, determination of Tehran Research Reactor Power was carried out (Armozd *et al*., 2011) using the method of ^{16}N gamma activity by detecting and counting the emitted gamma. The results obtained confirmed that the number of emitted gamma is proportional to the change in reactor power and can be applied to give reliable results for reactor power above 20 kW. This inform our present use of dose rate measurements to predict NIRR-1 in-core power.

Reactor power measurement by gamma and neutron radiation in Heavy Water Zero Power Reactor (HWZPR) was recently investigated by Jalali *et al*. (2013). Results show that the intensities of distributed gamma rays and neutrons from the reactor core are proportional to the reactor power, and the reactor calibrated power by this technique is on-line, prompt, and independent of safety and control rods and fuel configuration of the reactor with a good efficiency.

The behavior of reactor power level and flux with changes in core-coolant temperatures for a MNSR facility was investigated at two power levels using NIRR-1

(Ahmed *et al*., 2008). The methods used was a thermal hydraulic parameter by exploiting the core coolant temperature values and neutronic parameter. Results show that the semi-empirical relationship based on thermal hydraulics data and neutronic parameters could be used to predict the reactor's operating power. In addition, the measured data indicate that the reactor's operating power level can be estimated from the preset thermal neutron flux value. The measured data shows that there is a strong dependence of the reactor power on coolant temperature in agreement with the design of MNSR.

Recently, Ahmed *et al*. (2011) measured the core excess reactivity using the method of control rod critical depth of insertion and obtained the power and maximum operable time of NIRR-1. The result shows that there is a strong correlation between the reactor's operating time and its coolant temperature with the core excess reactivity. At 3.77 mk excess reactivity it was observed that for a full-power flux with the control rod position fully removed, the reactor operated for five continues hours. At half-power and under the same excess reactivity condition, the reactor reaches 8 h before the temperature effects sets-in. They reported that re-measurements done in 2009 by the staff of Centre for Energy Research and Training (CERT) shows that excess reactivity of the reactor has reduced to 2.80 mk, the operable time at full flux dropped to 3.5 h while that of half-power became 7 h. They also observed that the reactor's fluence depletion over the period under review was directly related to the excess reactivity reduction and therefore concluded that for a clean core excess reactivity of 3.77 mk, 5 and 8 h are the optimum times for the operation of miniature neutron source reactors under the two flux conditions (full and half power, respectively). As demonstrated in the study, a deviation from these optimum times is an indication of a drift in the reactor's core excess reactivity and hence the need to add beryllium shims to compensate for the loss.

Determination of radial and axial neutron flux distribution in irradiation channel of NIRR-1 using foil activation technique was carried out by Musa *et al*., (2012). The results show that for a preset neutron flux of 5.0 x 10^{11} $cm^{-2}s^{-1}$ the axial and radial neutron flux of NIRR-1 ranges from 4.47 x 10^{11} to 5.16 x 10^{11} $cm^{-2}s^{-1}$ and 4.80 x 10^{11} to 5.55 x 10^{11} $cm^{-2}s^{-1}$ respectively, with mean value of 4.79 x 10^{11} $cm^{-2}s^{-1}$ for axial and 4.99 x 10^{11} $cm^{-2}s^{-1}$ for radial, which were then compared with the previous measured values after commissioning of NIRR-1 and the one done recently at the Ghana MNSR. The values all pointed towards a level of consistency in variation despite the recent installation of cadmium-lined irradiation channel in NIRR-1, which is an indication that the installed cadmium line did not affect NIRR-1 flux stability. However, they reported that the individual foils shows slight flux variation from one foil position to another in the same irradiation container as against the claims of MNSR manufacturers and some users for perfect flux stability across the container, and concluded that, there is need for flux corrections to be made by MNSR users during NAA particularly for samples in the axial position instead of assuming a steady and constant flux throughout an irradiation container.

CHAPTER TWO
LITERATURE REVIEW

2.1 NEUCLEAR CROSS SECTIONS AND NEUTRON FLUX

To determine the frequency of neutron interactions, it is necessary to describe the availability of neutrons to cause interaction and the probability of a neutron interacting with material. The availability of neutrons and the probability of interaction are quantified by the neutron flux and nuclear cross section (DOE, 1993).

2.1.1 Cross Sections

The different interactions between neutrons and nuclei can be described by the concept of cross sections (Lilley, 2001). The cross section for a given neutron - nucleus reaction is a measurement of the probability of that particular interaction. The cross section is a property of the target nucleus and the energy of the incoming neutron (Glasstone and Sesonske, 1994). The cross section for a neutron – nucleus interaction is called the microscopic cross section and is denoted σ. The microscopic cross section is measured in m^2. As the cross section of a single nucleus is very small, about the cross section area of the actual nucleus, a derived unit called barn (b) is commonly used, where 1barn = $10^{-28}m^2$.

Whether a neutron will interact with a certain volume of material depends not only on the microscopic cross section of the individual nuclei but also on the number of nuclei within that volume. Therefore, it is necessary to define another kind of cross section known as the macroscopic cross section and is denoted ∑. The macroscopic cross section (∑) is the probability of a given reaction occurring per unit travel of the neutron and is related to the microscopic cross section (σ) by the relationship shown below

$$\sum = N\,\sigma \qquad 2.1$$

Where:

$\sum$ =macroscopic cross section (m^{-1})

N = atom density of material (atoms/m^3)

σ = microscopic cross-section (m^2)

2.1.2 Neutron flux

Macroscopic cross sections for neutron reactions with materials determine the probability of one neutron undergoing a specific reaction per centimeter of travel through that material (DOE, 1993). If one wants to determine how many reactions will actually occur, it is necessary to know how many neutrons are traveling through the material and how many centimeters they travel each second. It is convenient to consider the number of neutrons existing in one cubic centimeter at any one instant and the total distance they travel each second while in that cubic centimeter. The number of neutrons existing in a cm^3 of material at any instant is called neutron density and is represented by the symbol n with units of neutrons/cm^3. The total distance these neutrons can travel each second will be determined by their velocity.

A good way of defining neutron flux (ϕ) is to consider it to be the total path length covered by all neutrons in one cubic centimeter during one second. Mathematically, this is the equation below

$$\phi = n\,v \qquad 2.2$$

Where:

ϕ = neutron flux (neutrons/cm^2-sec)

n = neutron density (neutrons/cm^3)

v = neutron velocity (cm/sec)

The term neutron flux in some applications (for example, cross section measurement) is used as parallel beams of neutrons traveling in a single direction. The intensity (I) of a neutron beam is the product of the neutron density times the average neutron velocity. The directional beam intensity is equal to the number of neutrons per unit area and time (neutrons/cm²-sec) falling on a surface perpendicular to the direction of the beam. One can think of the neutron flux in a reactor as being comprised of many neutron beams travelling in various directions. Then, the neutron flux becomes the scalar sum of these directional flux intensities. Macroscopic cross sections for neutron reactions with materials determine the probability of one neutron undergoing a specific reaction per centimeter of travel through that material. If one wants to determine how many reactions will actually occur, it is necessary to know how many neutrons are travelling through the material and how many centimeters they travel each second. Since the atoms in a reactor do not interact preferentially with neutrons from any particular direction, all of these directional beams contribute to the total rate of reaction. In reality, at a given point within a reactor, neutrons will be travelling in all directions (DOE, 1993).

2.1.3 REACTION RATE

In a nuclear reactor, the neutron density is n neutrons per unit volume. Neutrons travel with a speed v and their interactions are described by macroscopic cross section ($\sum$). The number of interactions per unit volume and time is given by

$$R = n \cdot v \cdot \sum \qquad 2.3$$

Where R is the reaction rate (Lilley, 2001). The product $n \cdot v$ is an important quantity in reactor physics and is also written as

$$\phi = n\,v \qquad 2.4$$

Where ϕ is the neutron flux, and usually given as neutrons/cm²·s. The reaction rate is proportional to the neutron flux, and the higher the neutron flux the more reactions will take place.

2.2 NUCLEAR FISSION

Nuclear fission is a process in which an atom splits and releases energy, fission products, and neutrons. The neutrons released by fission can, in turn, cause the fission of other atoms. In the fission reaction the incident neutron enters the heavy target nucleus, forming a compound nucleus that is excited to such a high energy level ($E_{exc} > E_{crit}$) that the nucleus "splits" (fissions) into two large fragments plus some neutrons (DOE, 1993). The fission process usually divides the nucleus into two fission fragments and two to three free neutrons, accompanied by gamma radiation which we seek to measure on the top surface of the reactor. If at least one of these free neutrons initiates another fission, we may have the start of a nuclear chain reaction where the fission process is self-sustaining (Lamarsh and Baratta, 2001). An example of a typical fission reaction using U-235 is shown below (CNSC, 2003):

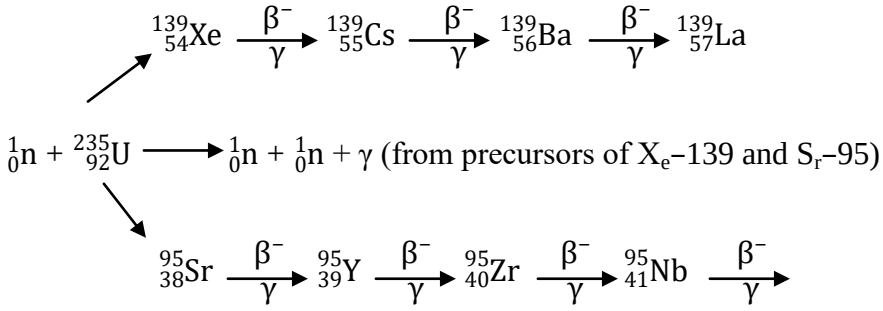

Fig. 2.1: Fission Product Decay Chain

The standard notation for the particular fission just described is as follows:

$$ {}^{1}_{0}\mathrm{n} + {}^{235}_{92}\mathrm{U} \rightarrow ({}^{236}_{92}\mathrm{U})^{*} \rightarrow {}^{139}_{54}X_e + {}^{95}_{38}S_r + 2({}^{1}_{0}\mathrm{n}) + \gamma \qquad 2.5 $$

After U-235 absorbs the neutron, the compound nucleus $({}^{236}_{92}\mathrm{U})^{*}$ survives for about 10^{-14}s, and then fission occurs about 85% of the time. (Radiative capture occurs about 15% of the time). The equation displays the immediate break up, with prompt neutrons and prompt gammas. Leaving out the compound nucleus simplifies the notation:

$$ {}^{1}_{0}\mathrm{n} + {}^{235}_{92}\mathrm{U} \rightarrow {}^{139}_{54}X_e + {}^{95}_{38}S_r + 2({}^{1}_{0}\mathrm{n}) + \gamma \qquad 2.6 $$

The energy release per fission, averaged over all fission reactions in a reactor core, is about 200 MeV (corresponding to a mass loss of nearly 0.2 u). This is, coincidently, approximately the energy per fission deposited in the reactor core. Individual fission reactions usually do not deviate from 200 MeV by more than a couple MeV. About 180 MeV of the energy release occurs at the moment of fission, the moment displayed in the notation just given. The beta emissions that follow release the remaining energy. Table 2.1 shows the distribution of energy released over the reaction products, and shows the energy deposition in the core (CNSC, 2003).

Table 2.1: Approximate Energy Distribution Resulting from a Typical U-235 Fission

Energy Source	Energy Released	Energy Deposited in Core	
	Energy (MeV)	Energy (MeV)	Energy (%)
Kinetic energy of lighter fission fragment	100 MeV	100 MeV	50%
Kinetic energy of heavier fission fragment	67 MeV	67 MeV	33.5%
Kinetic energy of fission neutrons	5 MeV	5 MeV	2.5%
Energy of prompt gamma rays	6 MeV	6 MeV	3%
Radiative capture of excess fission neutrons	—	8 MeV	4%
Beta particle energy gradually released from fission products	22 MeV (shared by β^- particles, gamma rays and neutrinos)	8 MeV	4%
Gamma ray energy gradually released from fission products		6 MeV	3%
Neutrinos		—	—
Total	200 MeV	200 MeV	100%

The energy released is given by the mass difference between the initial nucleus and the resulting fission fragments, and is given by Einstein's formula

$$E = \Delta mc^2 \qquad 2.7$$

Where Δm is the mass defect and c is the speed of light. The average energy release caused by fission of a heavy nucleus is about 200 MeV (Glasstone and sesonske, 1994).

2.3 NEUTRON MODERATION

The probability that a neutron will cause fission in fissile materials increases with decreasing neutron energy. It is therefore beneficial to slow down neutrons. The process of slowing them down is called moderation. Moderation is achieved by exposing a neutron to a series of scattering reactions, in which the neutron loses some of its kinetic energy in each collision. After a number of collisions the kinetic energy of the neutron is reduced to the average kinetic energy of the atoms in the scattering medium. The neutron is then in thermal equilibrium with the scattering medium, and is thus called a thermal neutron (i.e. the neutron is thermalized) (Glasstone and sesonske, 1994). Neutrons lose their energy most efficiently when colliding with light elements such as hydrogen, beryllium and carbon (Lilley, 2001). Common moderating materials are thus water, heavy water and graphite. Water and heavy water are the most popular moderators because they also function as coolant (Lamarsh and Baratta, 2001).

The moderator-to-fuel ratio (N^m/N^u), is very important in the discussion of moderators. As the reactor designer increases the amount of moderator in the core (that is, N^m/N^u increases), neutron leakage decreases. Neutron absorption in the moderator (Σ_a^m) increases and causes a decrease in the thermal utilization factor. Having insufficient moderator in the core (that is, N^m/N^u decreases) causes an increase in slowing down time

and results in a greater loss of neutrons by resonance absorption which also causes an increase in neutron leakage.

In practice, water-moderated reactors like NIRR-1 are designed with a moderator-to-fuel ratio so that the reactor is operated in an under moderated condition. The reason that some reactors are designed to be under moderated is if the reactor were over moderated, an increase in temperature would decrease the N^m/N^u due to the expansion of the water as its density became lower. This decrease in N^m/N^u would be a positive reactivity addition, increasing k_{eff} and further raising power and temperature in a dangerous cycle. If the reactor is under moderated, the same increase in temperature results in the addition of negative reactivity, and the reactor becomes more self-regulating (DOE, 1993).

2.4 RESEARCH REACTORS

Devices that are designed so that the fission chain reaction can proceed in a controlled manner are called nuclear reactors. In a reactor, this control is accomplished by varying the value of multiplication factor k, which can be done by the person operating the system. To increase the power being produced by a reactor, the operator increases k to a value greater than unity so that the reactor becomes supercritical. When the desired power level has been reached, he returns the reactor to critical by adjusting the value of k to be unity, and the reactor then maintains the specified power level.

To reduce power or shut the reactor down, the operator mainly reduces k, making the reactor subcritical. As a result, the power output of the system decreases. Nuclear bombs and explosives cannot be controlled in this way, and these devices are not referred to as reactors (Lamarsh and Baratta, 2001). To make a reactor critical, or otherwise to adjust the value of k, it is necessary to balance the rate at which neutrons are produced within the

reactor with the rate at which they disappear. Neutrons can disappear in two ways as the result of absorption in some type of nuclear reactor, or by escaping from the surface of the reactor (Lamarsh and Baratta 1982).

Research reactors are simpler than power reactors and operate at lower temperatures. They need far less fuel, and far less fission products build up as the fuel is used. On the other hand, their fuel requires more highly enriched uranium, typically up to 20% U-235, although some older ones use 93% U-235. They also have a very high power density in the core, which requires special design features. Like power reactors, the core needs cooling, though only the higher-powered test reactors need forced cooling. Usually a moderator is required to slow down the neutrons and enhance fission. As neutron production is their main f unction, most research reactors also need a ref lector to reduce neutron loss from the core (Krull, 2000).

There is a much wider array of designs in use for research reactors than for power reactors, with different operating modes, and producing energy which may be steady or pulsed. A common design is the pool type reactor, where the core is a cluster of fuel elements sitting in a large pool of water. Among the fuel elements are control rods and empty channels for experimental materials. Each element comprises several curved aluminium-clad fuel plates in a vertical box. The water both moderates and cools the reactor, and graphite or beryllium is generally used for the reflector, although other materials may also be used. Apertures to access the neutron beams are set in the wall of the pool (Krull, 2000).

2.5 NIRR-1 RESEARCH REACTOR DESCRIPTION

The Nigeria Research Reactor-1 (NIRR-1) is a Miniature Neutron Source Reactor (MNSR) designed by China Institute of Atomic Energy (CIAE) (Zhou, 1985) with under-moderation achieved by using a fuel material of highly enriched uranium and light water as moderator and coolant (Zhu, 1990; Azande *et al*., 2010). The reactor's first criticality was achieved on the 3rd of February 2004 (Balogun *et al*., 2004) and has since then been operating safely for neutron activation analysis (Jonah *et al*., 2005, 2006). NIRR-1 has a tank-in-pool structural configuration and a nominal thermal power rating of 31 kW. The current core of the reactor is a 230 mm×230 mm square cylinder and fuelled by U-Al4 enriched to 90.2% in Al-alloy cladding. It has a total number of 347 fuel pins and three Al dummies in the fuel lattice. The length of the fuel element is 248 mm, the active length being 230 mm with 9 mm Al-alloy plug at each end. The diameter of the fuel meat is 4.3 mm and the 235U loading in each fuel element is about 2.88 g. The cladding is Al-alloy, whose thickness is 0.6 mm. There is only one control rod in NIRR-1 serving as shim rod, regulation rod as well as safety rod. The functions of reactor start-up, steady state operation, and shutdown are accomplished by moving the control rod. The control rod is made up of a cadmium absorber 266 mm long and 3.9 mm in diameter with stainless steel of 0.5 mm thickness as the cladding material. The overall length of the CR is 450 mm in length (Ahmed *et al*., 2011).

One basic feature of NIRR-1 is the inherent safety due to limited core excess reactivity with a built-in clean cold core excess reactivity of 3.77mk measured during the on-site zero power and criticality experiments, the reactor can operate for a maximum of 4.5 hours at full power, mainly due to the large negative temperature feedback effects. Under these conditions, with the same fuel loading, the reactor can run for over ten years

with a burn-up of <1% (Jonal *et al*., 2007). An MCNP model of the reactor fueled with HEU has been developed and benchmarked by measured data obtained during the onsite zero power and power rising experiments (SAR, 2005). Fig. 2.2 shows a schematic diagram of the NIRR-1 (MNSR).

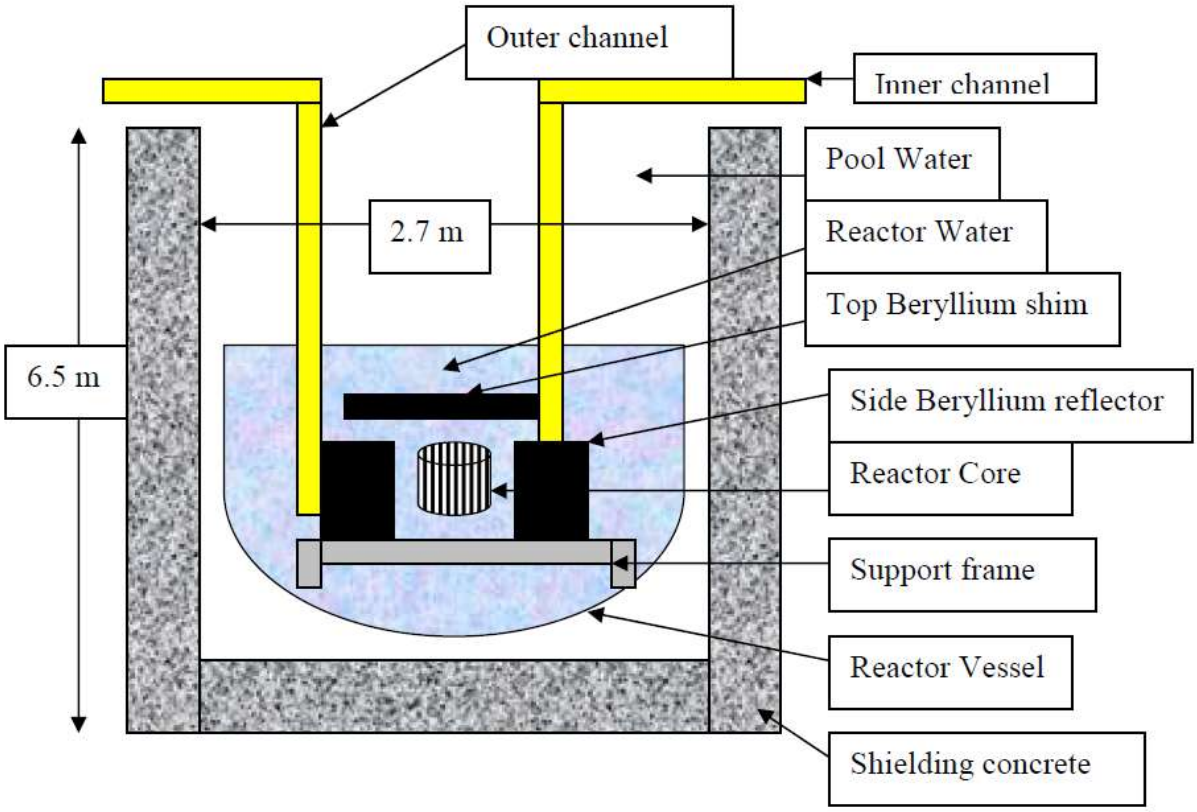

Fig. 2.2: Schematic diagram of MNSR (Ahmed *et al.*, 2008)

2.5.1 SAFETY FEATURES OF NIRR-1 REACTOR

The major safety feature of the reactor is its power self-limiting capability due to its negative temperature coefficient of reactivity. Increase in temperature coefficient leads to negative reactivity (a designed safety feature) (DOE, 1993).

The NIRR-1 is designed to include some inherent safety measures in order to prevent radiation leakage. The objective of its design is to achieve a minute core structure with under moderation, achieved by choosing highly enriched uranium as fuel material with light water serving as both moderator and coolant (Zhu, 1990; Azande *et al*., 2010). The core structure of the reactor was simplified by arranging the irradiation sites in and just after the beryllium reflectors. This has reduced the effect of the control rod movement on the reactivity and flux distribution in all the irradiation sites (Balogun, 2004), thus, enhancing the performance of the reactor from both mechanical and computational physics points of view.

To enhance safety, two major factors were also considered by the manufacturers of MNSR during construction and zero power experiments:

First, the ratio of hydrogen to uranium atoms was chosen to be 197 (Zhu, 1990) in order to enlarge the degree of under-moderation of the core and thereby increase its negative temperature coefficient of reactivity and to enhance the temperature feedback.

Second, the ratio of the core height to diameter was optimized to 1.0 (Guo, 1983). This is to enlarge the worth of the top beryllium reflector and thereby extend the lifetime of the core. It also facilitates the flow and mixing of the inlet and outlet coolants thus shortening the time of the temperature feedback.

Also, the optimization of the core height to unity increases the coupling of outlet and inlet mixing of the water coolant and enables part of the warm coolant to enter the core directly, thereby shortening the time of the temperature feedback.

The removal of heat from the core is achieved by natural convection and water recirculation. The coolant flow is at the transitional state from laminar to turbulent. The characteristic of the circulation was ascertained by computer codes (Guo, 1983; Shi, 1990) and thermal hydraulics simulation tests (Zhang, 1984). Safety experiments by Zhu (1990) and Akaho *et al*. (2000) shows that for the thermal hydraulics design to yield the desired rise in temperature, the height of inlet orifice for MNSR must remain at 6 mm and that of the outlet at 7 mm.

2.6 TRANSIENT CHARACTERISTICS OF NIRR-1

According to the design requirements, the NIRR-1 is a reactor with natural circulation cooling, self-stable by negative reactivity feedback. Therefore, the demonstration of its safety features during the positive reactivity insertion transient is very important. Theoretically, the kinetic transient is a physics thermo hydraulics-coupled problem, besides the neutronics response. That the moderator mass, momentum and energy conservation and various hydraulic flow resistances should be taken into account.

The NIRR-1 is cooled by natural circulation (i.e. thermal siphon) to remove the fission energy in the core, the cool water is sucked up through the inlet orifice formed between the side Be annulus and the bottom Be plate and flowing upward to wash the fuel elements. After being heated, the water flows out of the core through the outlet orifice formed between the top Be shim tray and the side Be annulus. The heat that the warm water

carries then is conducted to the pool water through the wall of upper and lower sections of the reactor vessels. Finally, the heat is dispersed into the environment.

2.7 REACTIVITY COEFFICIENTS

Changes in the physical properties of the materials in the reactor will result in changes in the reactivity. Reactivity coefficients are useful in quantifying the reactivity change that will occur due to the change in a physical property such as the temperature of the moderator or fuel (DOE, 1993).

The change in reactivity per degree change in temperature is called the temperature coefficient of reactivity. Because different materials in the reactor have different reactivity changes with temperature and the various materials are at different temperatures during reactor operation, several different temperature coefficients are used. Usually, the two dominant temperature coefficients are the moderator temperature coefficient and the fuel temperature coefficient.

2.7.1 MODERATOR TEMPERAURE COEFFICIENT

The temperature coefficient of reactivity is a very important safety parameter of research reactors. Many parameters that determine the multiplication factor depend on temperature. As a result, a change in temperature leads to a change in multiplication factor (k) and alters reactivity of the system (Lamarsh, 1982). A negative temperature coefficient of reactivity is desirable since it tends to counteract the effects of transient temperature changes during reactor operation. In MNSR reactors such as the NIRR-1 the moderator is the hydrogen that is mixed with the fuel itself. If the fuel temperature increases when the control rods are suddenly removed, the neutrons inside the hydrogen-containing fuel rod

become warmer than the neutrons outside in the cold water. These warmer neutrons inside the fuel cause less fissioning in the fuel and escape into the surrounding water. The end result is that the reactor automatically reduces the power within a few thousandths of a second, faster than any engineered device can operate. The inherent safety of the NIRR-1 reactor arises from the prompt negative temperature reactivity coefficient, whose measured value effectively limits the power when excess reactivity is suddenly inserted. The prompt temperature coefficient refers only to fuel temperature, and the overall temperature coefficient of the reactor refers to the change in the total core temperature.

Prompt and inherent reactivity feedbacks are considered important factors for research reactor safety (Akaho *et al*., 2002). For the MNSR such as the NIRR-1 reactor, inherent safety features are provided in their design since they are built with a negative Reactivity Temperature Coefficient (RTC). The mechanisms that affect reactivity in NIRR-1 reactor are the fuel and moderator expansion, void production among others. The reactivity due to temperature feedback $\rho(t)$ is expressed as (Akaho et al 2002)

$$\rho(t) = \rho_o(\mathrm{t}) + \alpha_M \Delta T_M(\mathrm{t}) + \alpha_F \Delta T_F(\mathrm{t}) \qquad 2.8$$

Where $\rho_o(\mathrm{t})$ is the initial reactivity, α_M and α_F are the moderator and fuel temperature coefficients of reactivity respectively. ΔT_M and ΔT_F are the deviation spatially averaged moderator and fuel temperatures from the equilibrium temperatures respectively. For MNSR such as NIRR-1 reactor, the core temperature of reactivity α_T is given by the addition of moderator and fuel temperature coefficient (Mirza *et al*., 1996; Akaho *et al*., 2003)

$$\alpha_T = \alpha_F + \alpha_M \qquad 2.9$$

The extent to which the reactivity is affected by changes in temperature is described in terms of the temperature coefficient of reactivity, denoted as α_T. It is defined as the change in reactivity with respect to temperature and is expressed as (Erradi *et al*., 2003)

$$\alpha_T = \frac{d\rho}{dT} \qquad 2.10$$

Where, reactivity which is the fractional departure of a system from criticality is expressed as (Lamarsh and Baratta, 1982)

$$\rho = \frac{k-1}{k} \qquad 2.11$$

Where, k is the multiplication number.

Differentiating equation (2.11) gives

$$\alpha_T = \frac{1}{k^2}\frac{dk}{dT} \qquad 2.12$$

In all cases of interest k is close to unity and so equation (2.12) can be written approximately as

$$\alpha_T = \frac{1}{k}\frac{dk}{dT} \qquad 2.13$$

Equation (2.11) is more convenient than equation (2.10) for calculation purpose and is often taken as the definition of α_T. According to equation (2.13), α_T is equal to the fractional change in k per change in temperature and has units of $(\text{degrees})^{-1}$

The response of reactor to a change in temperature depends on the algebraic sign of coefficient of reactivity α_T.

Consider a situation when α_T is positive. Since k is always positive, $\frac{dk}{dT}$ is also positive, which means that an increase in T leads to an increase in k and so on. Now, suppose for some reason the temperature of the reactor increases. This increase the value of k, which in turn leads to an increase in the power level of the reactor giving rise to a further

increase in the temperature, another increase in k and so on. Thus, with α_T positive, an increase in temperature leads to ever increase in temperature and power until the reactor either shutdown by outside intervention or it melts down.

However, suppose the reactor temperature decreased, if α_T is positive a decrease in T leads to a decrease in k. This reduces the temperature, giving rise to a further decrease in k, and so on, until the reactor eventually shutdown. Thus, if $\alpha_T > 0$, an increase in T leads to meltdown, a decrease in T to shut down in the absence of external intervention.

The situation is quite different when α_T is negative. In this case, $\frac{dk}{dT}$ is negative, and an increase in T gives a decrease in k. Now an increase in reactor temperature leads to decrease in reactor power, which tends to decrease the temperature and return the reactor to its original state. Furthermore, a decrease in T results in an increase in k, so that if T goes down the power goes up and again the reactor tends to return to its original state. Clearly, a reactor with positive α_T is inherently unstable to changes in temperature, whereas a reactor having a negative α_T is inherently stable (Lamarsh and Baratta, 1982).

It should be noted that the temperature ordinarily does not change uniformly throughout a reactor. For instance, an increase in reactor power is reflected first by a rise in the temperature of the fuel since this is the region where power is generated. In a thermal reactor, the coolant and moderator temperatures do not increase until heat has been transferred from the fuel to these regions. It is important in discussing temperature coefficient to specify the component whose temperature is undergoing change. Thus, the fuel temperature coefficient is defined as the fractional change in k per unit change in fuel temperature. The moderator temperature coefficient is the fractional change in k per unit change in moderator temperature (Larmash and Baratta, 1982).

Because the temperature of the fuel reacts instantly to changes in reactor power, the fuel temperature coefficient is also called prompt temperature coefficient, denotes as α_{prompt} (lamarsh and Baratta, 1982). The value of α_{prompt} determines the first response of a reactor to changes in either fuel temperature or reactor power. For this reason, α_{prompt} is the most important temperature coefficient insofar as reactor safety is concerned.

In practice, control of a MNSR reactor such as the NIRR-1 reactor is enhanced by several negative feedback mechanisms relying on physical phenomena.

2.7.2 FUEL TEMPERATURE COEFFICIENT

Another temperature coefficient of reactivity, the fuel temperature coefficient, has a greater effect than the moderator temperature coefficient for some reactors. The fuel temperature coefficient is the change in reactivity per degree change in fuel temperature. This coefficient is also called the "prompt" temperature coefficient because an increase in reactor power causes an immediate change in fuel temperature. A negative fuel temperature coefficient is generally considered to be even more important than a negative moderator temperature coefficient because fuel temperature immediately increases following an increase in reactor power. The time for heat to be transferred to the moderator is measured in seconds. In the event of a large positive reactivity insertion, the moderator temperature cannot turn the power rise for several seconds, whereas the fuel temperature coefficient starts adding negative reactivity immediately (DOE, 1993).

2.8 FUEL BURNUP

The initial fuel load of a new reactor is entirely fresh fuel, that is, fuel with no plutonium or fission products present. Poison in the moderator compensates for the excess reactivity of this fuel in the first few months of operation. Exposure to neutron flux gradually changes the composition of the fuel, a process known as fuel burnup. After four to six months of operation at high power, core reactivity drops to a level where a poison shim is no longer required and routine replacement of fuel becomes necessary to maintain core reactivity. The reactor is then described as equilibrium-fuelled. Fuel is replaced on a daily basis (between 8 and 18 bundles per day) to add reactivity at a rate equal to its rate of loss from burnup.

In a freshly fuelled bundle, the only fissile material is U-235, which constitutes 0.72% of the natural uranium. Exposure to neutron flux gradually depletes the U-235, decreasing reactivity. Buildup of the fission products, especially those with significant absorption cross-sections for thermal neutrons further reduces reactivity. These losses are only partly compensated by the buildup of fissile Pu-239 following neutron radiative capture in U-238 (producing U-239, which subsequently decays to Np-239, followed by a second beta decay to Pu-239). Similarly, the net effect of Pu-240 and Pu-241 buildup is a net loss in reactivity. Eventually, the gradual change in fuel composition requires replacement of the high burnup fuel with fresh fuel to maintain the core critical (CNSC, 2003).

2.8.1 BURNUP RATE 0F U-235

The fuel loses one U-235 atom whenever a U-235 nucleus absorbs a neutron. The rate of absorption decreases as the U-235 concentration drops and this produces a characteristic exponential drop in U-235, as Figure 2.3 shows. The removal rate (slope of the curve) is highest when there is the most U-235, and decreases as U-235 decreases (CNSC, 2003).

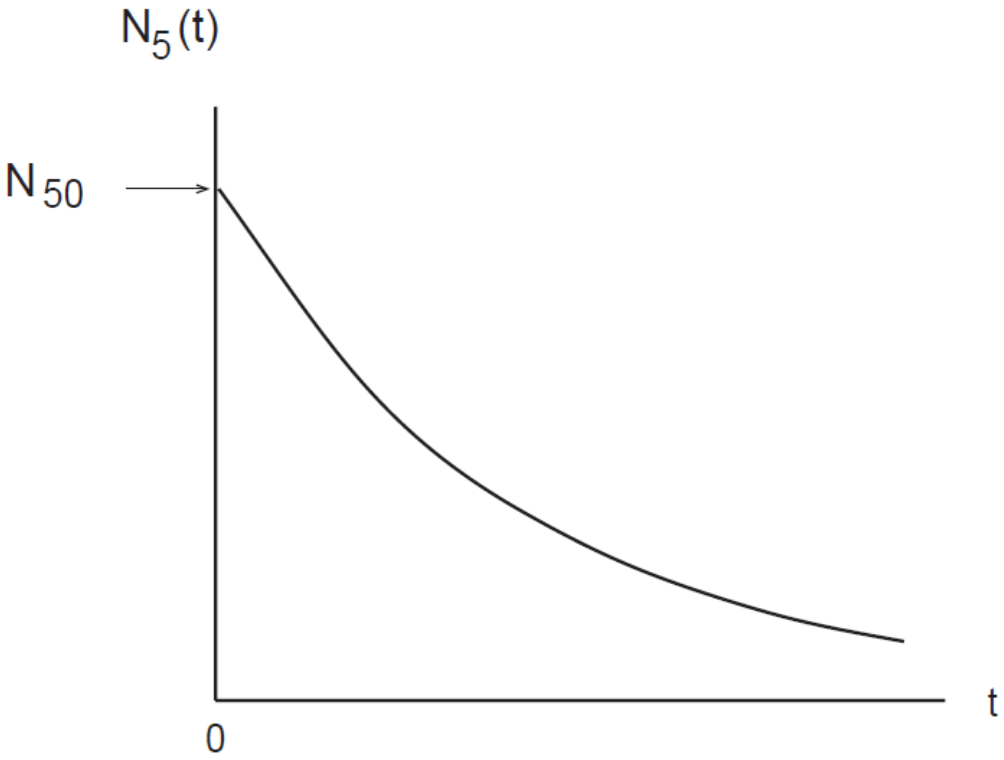

Fig. 2.3: Exponential Decrease in U-235 Concentration

We can see how this behavior occurs by looking at the removal process. Neutron absorption removes U-235 from the fuel at the rate $R_a = \phi\Sigma_a^5 = \phi N_5\sigma_a^5$. We write this as:

$$\frac{dN_5}{dt} = -(\sigma_a^5\phi)\, N_5 \qquad 2.14$$

Where N_5 is the number of U-235 nuclei per cm^3,

σ_a^5 is the microscopic absorption cross-section of U-235 (in cm^2),

ϕ is the neutron flux in n/cm^2s.

The negative sign on the right hand side accounts for the fact that N_5 is decreasing.

This equation is of the same form as the radioactive decay equation:

$$\frac{dN}{dt} = -\lambda N \qquad 2.15$$

Where the product $(\sigma_a^5\phi)$ in the burnup equation is equivalent to the decay constant λ in the decay equation, provided ϕ is constant. The U-235 concentration therefore decreases in exponential fashion, as Figure 2.2 shows. It typically drops to about 1/4 of its initial value of 0.72% by the time the fuel is discarded.

The equation for U-235 concentration is

$$N_5(t) = N_{50}\, e^{-(\sigma_a^5\phi)t} \qquad 2.16$$

Where N_{50} is the value of N_5 at time $t = 0$.

2.9 REACTOR DYNAMICS

When power changes in a reactor are large enough to influence the value of the reactivity, the transient behavior of the reactor is termed as the reactor dynamics. As can be expected, the influence of power on the reactivity has to be quantified in order to properly describe the dynamic behavior of the reactor (Alhassan, 2009).

During operation of a reactor the energy released due to nuclear fission is deposited to the coolant. The resulting temperature distribution in the fuel and coolant (in BWRs even the void fraction distribution) is a subject of the thermal-hydraulic analysis of the reactor. The temperature distribution, which in a general case is a function of both the time and the location, is influencing the values of microscopic cross-sections for various nuclear reactions caused by neutrons. As a result the reactivity will depend on the temperature changes.

From a practical point of view it is important to know what the influence of temperature on reactivity is and how it will influence the operation of the nuclear reactor. In general the following two cases can be considered:

i. Reactivity increases with the temperature: in this case the increasing reactivity will cause the increase of the reactor power, which, in turn, will cause the increase of temperature, etc. That means in this case the reactor will be inherently unstable.

ii. Reactivity decreases with temperature: in this case the decreasing reactivity will cause the decrease of the reactor power which will be followed by the decrease of the temperature, and so on. Clearly the reactor will be inherently stable in such a case.

The conclusion is that reactors should be constructed in such a way which assures the decreasing reactivity in function of temperature. This can be achieved by using proper materials and a proper nuclear reactor configuration. The reactivity changes with temperature because the reactivity depends on macroscopic cross sections, which themselves involve the atomic number densities of materials in the core (Alhassan, 2009).

2.10 DYNAMIC FEEDBACK CHARACTERISTICS OF NIRR-1

NIRR-1 has the following characteristic. If the output power increases, the reactivity becomes negative and the reactor tends to decrease the output power. If the output power decreases, the reactivity becomes positive and the reactor tends to increase the output power. In other words, the output of the NIRR-1 reactor exhibits negative feedback. The magnitude of the feedback changes over a wide range by the design of the reactor. The reactor fuel contains fissile material and fertile material. The fertile material has large resonance absorption. Because of this large absorption, the neutron spectrum (neutron flux) has a sharp dip at this energy. Therefore, the number of absorbed neutrons decreases compared to a flat neutron spectrum. This is called self-shielding. If the output power and temperature increase, the thermal motion of fuel will intensify. Thus, when a neutron in motion with a constant energy *E* collides with a fuel nucleus, the energy should be modified by the thermal motion of the nucleus. This means that the resonance of the cross-section widens, while the area stays constant. Thus, the peak of the cross-section decreases, the self-shielding effect is reduced, and absorption increases. This is a negative feedback for U-238 capture resonance

In practice, water-moderated reactors such as the NIRR-1 are designed with a moderator-to-fuel ratio so that the reactor is operated in an under moderated condition. The reason that some reactors are designed to be under moderated is if the reactor were over moderated, an increase in temperature would decrease the moderator to fuel ratio (N^m/N^u) due to the expansion of the water as its density became lower. This decrease in N^m/N^u would be a positive reactivity addition, increasing k_{eff} and further raising power and temperature in a dangerous cycle. If the reactor is under moderated, the same increase in

temperature results in the addition of negative reactivity, and the reactor becomes more self-regulating (DOE, 1993).

2.11 STATISTICAL PACKAGE FOR THE SOCIAL SCIENCES (SPSS)

The statistical package for the social sciences (SPSS) is a software package used for conducting statistical analysis, manipulating data, and generating table and graphs that summarize data (Ravishankar and Dey, 2002). SPSS performs statistical analysis range from basic descriptive statistics, such as average and prevalence, to advanced inferential statistical, such as regression model, analysis of variance (ANOVA), factor analysis etc. SPSS also contains several tools for manipulating data, including functions for recording data, macros programming on visual basic editor, merging data, and aggregating complex data sets (Kutner *et al.,* 2004). Before SPSS, researchers had to run statistical tests on data sets by hand. However, SPSS automates this process.

- Data Collection and Organization

SPSS is often used as a data collection tool by researchers. The data entry screen in SPSS looks much like any other spreadsheet software. You can enter variables and quantitative data and save the file as a data file. Furthermore, you can organize your data in SPSS by assigning properties to different variables. For example, you can designate a variable as a nominal variable, and that information is stored in SPSS. The next time you access the data file, which could be weeks, months or even years, you'll be able to see exactly how your data is organized.

- Data Output

Once data is collected and entered into the data sheet in SPSS, you can create an output file from the data. For example, you can create frequency distributions of your data to determine whether your data set is normally distributed. The frequency distribution is displayed in an output file. You can export items from the output file and place them into a research article you're writing. Therefore, instead of recreating a table or graph, you can take the table or graph directly from the data output file from SPSS.

- Statistical Tests

The most obvious use for SPSS is to use the software to run statistical tests. SPSS has all of the most widely used statistical tests built-in to the software. Therefore, you won't have to do any mathematical equations by hand. Once you run a statistical test, all associated outputs are displayed in the data output file. You can also transform your data by performing advanced statistical transformations. This is especially useful for data that is not normally distributed.

2.11.1 REGRESSION ANALYSIS

In statistics, regression analysis is a statistical process for estimating the relationships among variables. It includes many techniques for modeling and analyzing several variables, when the focus is on the relationship between a dependent variable and one or more independent variables (or 'predictors'). More specifically, regression analysis helps one understand how the typical value of the dependent variable changes when any one of the independent variables is varied, while the other independent variables are held

fixed. Most commonly, regression analysis estimates the conditional expectation of the dependent variable given the independent variables-that is, the average value of the dependent variable when the independent variables are fixed. Less commonly, the focus is on a quantile, or other location parameter of the conditional distribution of the dependent variable given the independent variables. In all cases, the estimation target is a function of the independent variables called the regression function (Scott, 2012). In regression analysis, it is also of interest to characterize the variation of the dependent variable around the regression function which can be described by a probability distribution.

Many techniques for carrying out regression analysis have been developed. Familiar methods such as linear regression and ordinary least squares regression are parametric, in that the regression function is defined in terms of a finite number of unknown parameters that are estimated from the data. Non parametric regression refers to techniques that allow the regression function to lie in a specified set of functions which may be infinite-dimensional (Freedman, 2005).

Simple linear regression is used to model the relationship between a single response variable, Y, and a single explanatory variable, X. The model is

$$Y = \beta_o + \beta_1 X_i + \varepsilon_i \qquad 2.17$$

where (Y_i, X_i), i = 1, …, n are the sample values of the response and exploratory variables and ε_i are random disturbance terms assumed to be normally distributed with mean zero and variance σ^2. The intercept parameter β_o is the value predicted for the response variable when the explanatory variable takes the value zero. The slope parameter β_1 is the change in the response variable predicted when the explanatory variable is increased by one unit. The

parameters, also known as regression coefficients, can be estimated by least squares (Landau and Everitt, 2004).

2.11.2 REGRESSION COEFFICIENT

Regression coefficient is a measure of how strongly each independent variable predicts the dependent variable. There are two types of regression coefficients. Unstandardized coefficients and standardized coefficients, also known as beta value. The unstandardized coefficients can be used in the equation as coefficients of different independent variables along with the constant term to predict the value of dependent variable. The standardized coefficients (beta) is however, measured in standard deviations (Gaur and Gaur, 2009). They are standardized so that they measure the change in the dependent variable in units of its standard deviation. The standardization enables the comparison of effects across explanatory variables.

These regression coefficients can be used to construct an Ordinary Least Squares (OLS) equation and also to test the hypotheses on each of the independent variables (Gaur and Gaur, 2009). Equation (2.18) shows a general Ordinary Least Squares (OLS) equation for a simple linear regression analysis (Landau and Everitt 2004).

$$Y = \alpha + \beta X \qquad 2.18$$

Where Y is the dependent variable, X is the independent variable, α is the constant term and β is the regression coefficient for the independent variable. The entered data set contains observations for Y and X. The parameters α and β are unobservable, and the task of regression analysis is to produce an estimate of these two parameters, based upon the information contained in the data set.

2.12 REACTOR POWER

Neutron power is essentially the fission rate multiplied by the prompt energy release per fission. We cannot measure this directly, but we can monitor the flux and the average neutron flux in the core is proportional to the overall fission rate.

Reactor thermal power (often shortened to thermal power) is the reactor's rate of heat energy production. Thermal power takes account of nuclear decay heating and of conventional heat (pump heat and heat losses to the environment).

Fission power is the name given to the heat generated because of nuclear processes in the fuel. This includes wasted heat, such as that generated in the moderator and shielding. It does not include any conventional heating. The operating license places an upper limit on fission power, which is enforced by regulating the reactor thermal power. For instance, the upper fission power for NIRR-1 considered in this work.

One fission releases 200 MeV or 3.2×10^{-11} J of recoverable energy. To produce 1 W requires fission of 3.12×10^{10} nuclei per second (Glasstone and Sesonske, 1994). By multiplying the average reaction rate with the reactor core volume and dividing by the number of fissions per second, we can determine the total power produced by the reactor:

$$P = \frac{V \cdot \Sigma_f \cdot \phi_{th}}{3.12\times10^{10}} \qquad 2.19$$

where P is the thermal output power in Watt, ϕ_{th} is the average thermal neutron flux in neutrons/cm^2 · s, $\sum_f$ is the average macroscopic cross section in cm^{-1} and V is the core volume given in cm^3 (Glasstone and Sesonske, 1994).

V and $\sum_f$ are fixed parameters for a given reactor. The power of the reactor is thus proportional to the average neutron flux ϕ, or vice versa.

2.12.1 REACTOR POWER LEVEL

A change in reactor power level can result in a change in reactivity if the power level change results in a change in system temperature. The power level at which the reactor is producing enough energy to make up for the energy lost to ambient is commonly referred to as the point of adding heat. If a reactor is operating well below the point of adding heat, then variations in power level produce no measurable variations in temperature. At power levels above the point of adding heat, temperature varies with power level. Decrease in reactor temperature leads to positive reactivity and increase in power level. Increase in reactor temperature leads to negative reactivity and decrease in power level near the point of adding heat to maintain system temperature. Some slight oscillations above and below the new power level occur before steady state conditions are achieved. The final result is that the average temperature of the reactor system is essentially the same as the initial temperature, and the reactor is operating at the new higher required power level (DOE, 1993).

2.12.2 REACTOR POWER MEASUREMENT BASES

In the fission process of heavy nuclei such as uranium and plutonium, two or three neutrons, six or seven gamma photons, six betas, six antineutrinos, two or three fission fragments are produced. They carry totally about 200 MeV of fission energy. In nuclear reactors, continuous induced fission process happens to sustain reactor criticality; therefore, the reactor is a powerful source of these particles. In the reactor criticality state, great mass of gamma photons and neutron particles are produced and distributed inside and outside of the reactor. Core gamma rays are produced and distributed during criticality from fission process, fission fragments, Bremsstrahlung process, Compton scattering, positron

annihilation and (n, γ), (n, pγ), (n, αγ), (n, 2nγ), (n, n′γ), … nuclear reactions in core compounds and the shielding around the core (Jalali *et al*., 2013). Fission process, fission fragments, photon–neutron reactions in the light water and (n, 2n), (n, n′) reactions with core materials are also neutron sources in LWZPR reactor. Fig 2.4 shows all reactions and how particles are produced within the reactor in the cascade process (Schaeffer, 1973; Glasstone and Sesonske, 1980). All reactions and produced particles change proportional to neutron flux or reactor power. Fission fragments and beta particles lose total energies while the neutrons and gamma rays lose a fraction of their energies within the reactor. But antineutrinos lose all of their energies outside of the reactor because of their low reaction cross-sections. From all these particles only neutrons have the principal and basic roles in the fission cycle process. All computations, designs, simulations, reactor parameters measurement are based on neutron reactions within the reactor core. Other particles have no important role in the reactor dynamic and static quantities. Particles other than neutrons have rarely been used in reactor parameters measurement. All particles produced in the reactor have been used for reactor power calibration and measurement.

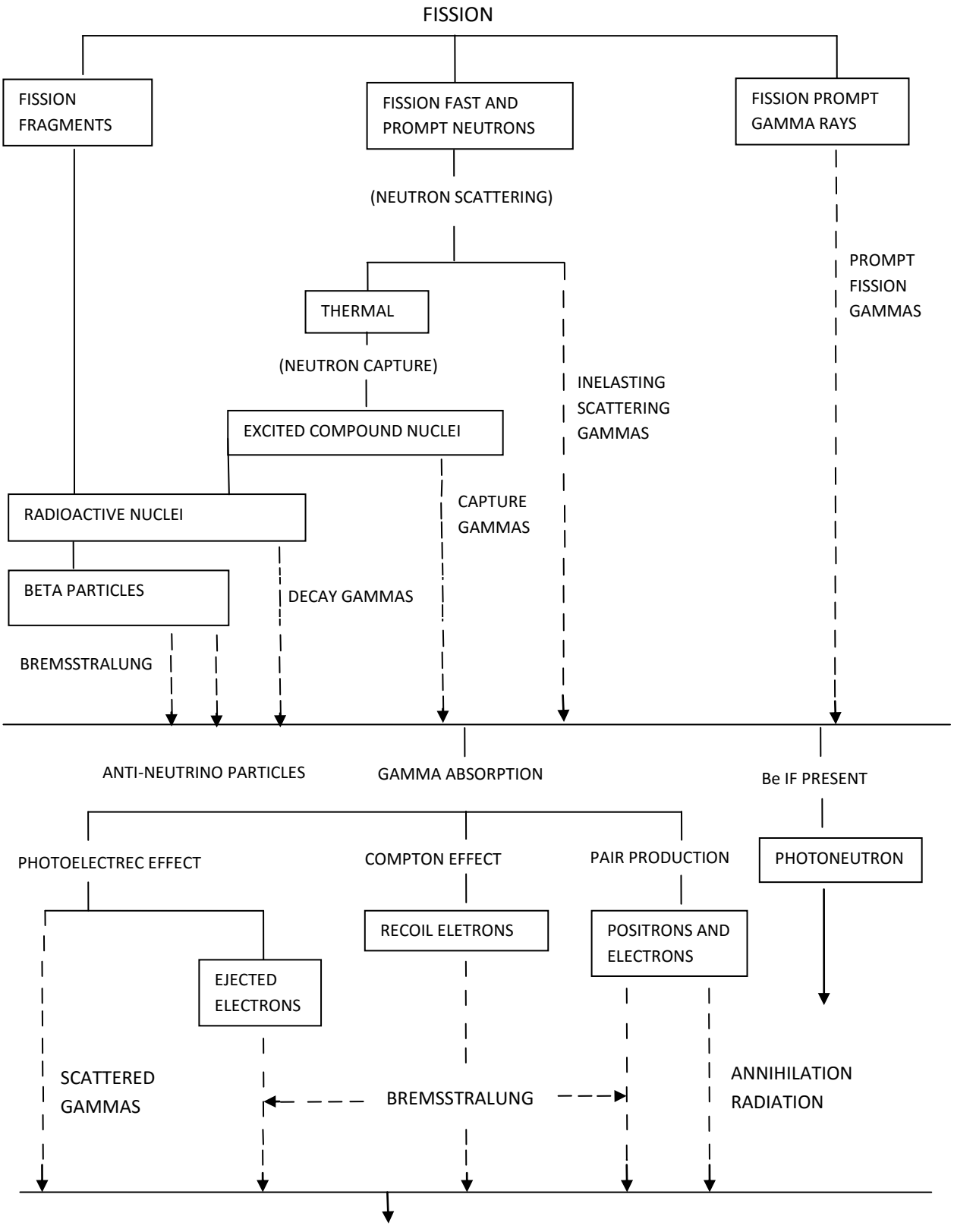

Fig. 2.4: Flow chart of a Nuclear reactor radiation particles structure

In Table 2.2, all reactor power measurement and calibration techniques have been compiled and summarized (Lu, 1964, Mogilner and Shvetsov, 1967, Letter to the editor, 1970, Klimov *et al*., 1994, Beeley *et al*., 1997, Yamamoto and Miyoshi, 1999, Shi and Li, 2001, Nishitani *et al*., 2002, Tsypin *et al*., 2003, Arakani and Gharib, 2009, Lhuillier, 2009, Sadeghhi, 2010, Coulon *et al*., 2011, Armozd *et al*., 2011 and Mesquita *et al*., 2011). In reactors whose power can warm the coolant or moderator, the use of calorimetric technique with or without flow is considered to be the best and the most complete method for reactor power measurement. Then all power measuring instruments such as Fission Chamber (FC), Compensated Ionization Chamber (CIC) and Uncompensated Ionization Chamber (UIC) are calibrated based on calorimetric technique. However, in low power reactors especially zero power reactors, microscopic nuclear techniques have been developed which are based on reactor dynamic and static equations and its solution techniques, neutron noise analysis, fission rate and neutron flux. In this paper, we give a method for power estimation based on simultaneous measurement of both neutron, temperature and gamma radiations emitted from the NIRR-1 reactor core.

Table 2.2: Nuclear reactor power measurement and calibration techniques

Technique	Reactor type	Application(absolute power measurement or calibration)	Measurement conditions
Calorimetric	Power, research	Absolute measurement	On-line
Intensity Cherenkov ray	Pool type research	Calibration	On-line, prompt, light water
Delayed neutron rate	Power, research	Calibration	On-line, delayed
Delayed gammas from ^{16}N $^{16}O(n,p)^{16}N$	Power, research	Calibration	On-line, delayed. Coolant light water reactor
Delayed gammas from ^{16}N, ^{18}F $^{16}O(n, p)^{16}N$, $^{18}O(p, n)^{18}F$	Research	Calibration	On-line, delayed, coolant light water
Delayed gammas from ^{20}F and ^{23}Ne	Fast reactor power, research	Calibration	On-line, delayed, coolant sodium reactor
Anti-neutrino electron	Power	Calibration	Off-site of reactors, online, prompt
In-direct fission rate measurement	Research	Calibration	Off-line, delayed, fission chamber
Direct fission rate measurement	Research low power	Absolute measurement	Off-line, delayed solid track detector
Fission fragments activity	Research	Absolute measurement	Off-line, delayed, ^{143}Ce activity
Standard neutron source	Research low power	Absolute measurement	On-line, prompt
Neutron flux mapping	Research	Absolute measurement	Gold foil activation, off-line, delayed
Rossi-Alpha statistical technique	Research	Absolute measurement	On-line, prompt
Feinman statistical technique	Research	Absolute measurement	On-line, prompt
P_0 statistical technique	Research	Absolute measurement	On-line, prompt
Differential statistical technique	Research	Absolute measurement	On-line, prompt
Frequency statistical technique	Research	Absolute measurement	On-line, prompt

2.12.3 MODERATOR TEMPERATURE DEPENDENT REACTOR POWER

The semi-empirical relation amongst core inlet temperature, coolant temperature rise and power levels as obtained from simulation experiments on MNSR is expressed in the form (Shi, 1990):

$$\Delta T = (5.725 + 147.6H^{-2.64})T_{in}^{-0.35} P^{(0.59+0.0019T_{in})} \quad 2.20$$

Where ΔT = Temperature difference between inlet and outlet orifices (°C)

H = Height of the inlet orifice (mm)

T_{in} = Inlet temperature (°C)

The designed inlet orifice of NIRR-1 was made to be 6 mm for safety and technical reasons (Yang, 1992). Therefore, substituting the value of H in to Eq. (2.20) reduces the equation to

$$\Delta T = 7.04T_{in}^{-0.35} P^{(0.59+0.0019T_{in})} \quad 2.21$$

The reactor power is thus given by

$$P = \text{Exp}\left[Ln\left(\frac{\Delta T}{7.04T_{in}^{-0.35}}\right)(0.59 + 0.0019T_{in})^{-1}\right] \quad 2.22$$

For a fixed height of inlet orifice, it is expected from Eq. (2.22) that the reactor power varies linearly with coolant temperature rise.

2.12.4 FLUX DEPENDENT REACTOR POWER

Apart from the above method of determining the reactor power via the thermal hydraulic parameters, the neutronic parameters (neutron flux values) could as well be exploited to predict the fission power of the reactor, as long as nuclear data parameters are accurately known (Ahmed *et al.,* 2006). The equation that relates these two parameters is:

$$P = 3.1x10^{-10}\sum_f V_f \phi \quad 2.23$$

Where ϕ = average thermal neutron flux in the inner irradiation channel ($ncm^{-2}s^{-1}$)

V_f = volume of the core = πr^2h (cm^3)

Core height (h) = 23 cm

Core radius (r) = 11.5 cm

$\sum_f$ = macroscopic fission cross-section of the core fuel = 1.013x10^{-2} cm^{-1}

A cylindrical core with a cross-sectional area of 23 cm² and highly enriched uranium (^{235}U) was used as fuel for the Nigeria MNSR. The above parameters make it possible to reduce Eq. (2.23) to only a flux dependent reactor power equation as shown in Eq. (2.24).

$$P = 3.0x10^{-8}\phi \quad (2.24)$$

Equation (2.24) reveals a linear relationship between the reactor power and its neutron flux. It shows that the reactor power could also be predicted from the experimental neutron flux values.

2.12.5 DOSE-RATE DEPENDENT REACTOR POWER

For the power-level prediction as a function of the measured dose-rate γ, the regression coefficients from equation (2.18) using the regression analysis over the whole reactor operating range can also be represented by the following Ordinary Least Squares (OLS) equation between neutron flux and dose-rate:

$$\phi = a + b \cdot \gamma \quad (2.25)$$

Where ϕ is the thermal neutron flux representing the dependent variable Y, a is a constant term and b the regression coefficient for the independent variable γ (X).

From Equations (2.24) and (2.25), the correlation between reactor power and the measured dose-rate becomes:

$$P = 3.0x10^{-8}\,(a + b \cdot \gamma) \quad (2.26)$$

Where P is the thermal power in watt and γ is the dose-rate in μSv/h.

2.12.6 DOSE-RATE AND AVERAGE CORE TEMPERATURE

Such measurements are accompanied with the measurement of both the inlet T_{in} and outlet T_{out} water temperatures of the core, and the temperature difference across the core ΔT. Then, a relationship between dose-rate and ΔT is established.

Knowing that the average core temperature is considered as the mean of the core inlet and outlet temperatures, it can be assumed that (Khamis and Jamal, 2006):

$$\overline{T_{core}} = T_{in} + \frac{\Delta T}{2} \qquad 2.27$$

Where $\overline{T_{core}}$ is the average core temperature (°c), T_{in} is the core inlet temperature (°c), and ΔT is the temperature difference across the core (°c).

From equations (2.21) and (2.27), the average core temperature as a function of reactor power is given as:

$$\overline{T_{core}} = T_{in} + \frac{7.04 T_{in}^{-0.35} P^{(0.59+0.0019 T_{in})}}{2} \qquad 2.28$$

Using equation (2.18) for the regression coefficients in the regression analysis, the following Ordinary Least Squares (OLS) equation between the coolant temperature rise and dose-rate can be constructed:

$$\Delta T = a + b \cdot \gamma \qquad 2.29$$

Where γ is the dose-rate on top of the reactor vessel, at the centerline of the reactor (μSv/h), a is a constant term and b the regression coefficient for the independent variable.

Using equations (2.27) and (2.29), the average core temperature as a function of dose-rate can be written as:

$$\overline{T_{core}} = T_{in} + \frac{a + b \cdot \gamma}{2} \qquad 2.30$$

CHAPTER THREE
MATERIALS AND METHOD

3.1 MATERIALS

The following materials were used to perform the experiments:

a. NIRR-1 (Designed: China Institute of Atomic Energy, No. 1): to perform the experiment.

b. Fission chamber (LB 1120): to measure the neutron flux.

c. Thermocouples (Nickel-Alumel/Nickel-Chromium): to measure the core inlet and outlet temperatures.

d. Geiger-Muller counter (Model: FJ-321CG5 transistor 4–channel γ monitor, Precision: ±10%): to measure the γ dose-rate.

e. Stop watch: to record the time.

f. Computer (PC, window 8) and SPSS statistics (IBM company, version 21): to perform the linear regression analysis.

3.2 EXPERIMENTAL PROCEDURE

3.2.1 Neutron flux measurement

A miniature fission chambers made using stainless steel walls and electrodes, with the operating voltage that varies from about 50 to 300 V was employed as neutron flux detector. Walls of the chambers are lined with highly enriched uranium to enhance the ionization current with argon as a common choice for the chamber fill gas used at a pressure of several atmospheres.

There are two small vertical holes each 10 mm in diameter and 190 mm deep on the side annular beryllium reflector on the same circle as the inner irradiation sites (i.e. on a

circle of radius 165 mm and at angles of 144^0 to each other). A current-type miniature fission chamber (LB 1120) is placed in each hole to monitor neutron flux at each irradiation site and provide control signals. The locations of the neutron flux detectors (fission chambers) are shown in Fig. 3.1. The sensitivity and linearity of the miniature fission chambers are adequate to measure NIRR-1 neutron flux, and has good tightness, with hard cable being used to enable it work in the water pool and at high environmental temperature.

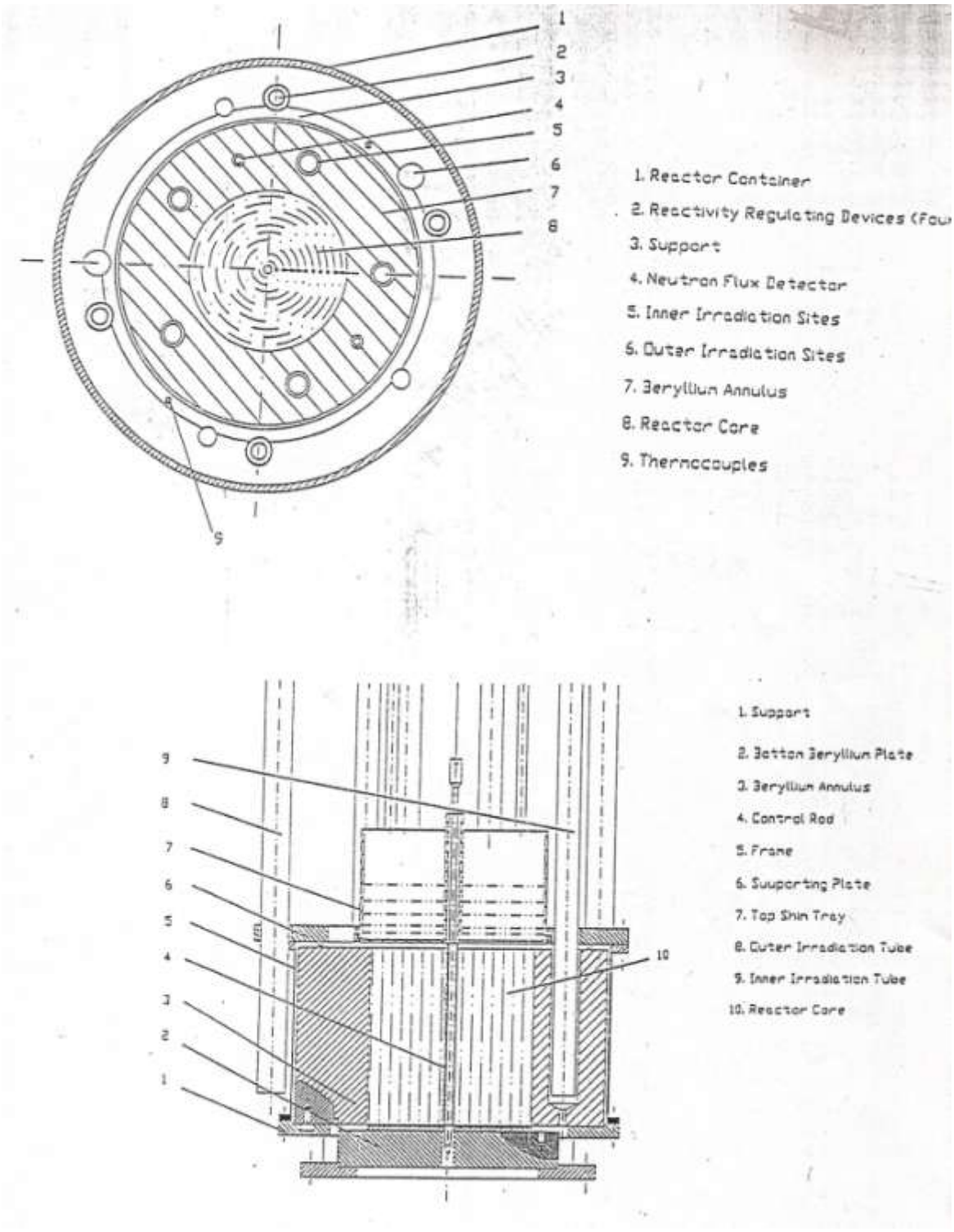

Fig. 3.1: Sectional views of Reactor Vessel and other components (SAR, 2005)

The principle for measuring thermal neutron flux with miniature fission chamber is as follows: When thermal neutron hit the U-235 coating of the fission chamber, fission reaction takes place. The fission fragments ionized the filled gas, and ion pairs are produced. The fission fragments, being massive charged particles with Z≈+20*e* and kinetic energy 60-100Mev, have a short range even in a gas and produced an intense ionization to the extent that gas multiplication is not necessary. Under the action of electric field, positive and negative ion pairs move towards the electrodes, thus a mean current $\bar{I}_n$ is formed in the external circuit. The relation of $\bar{I}_n$ and the in-pile neutron flux is expressed as $\bar{I}_n = S_{In}\ \bar{\phi}_n$, where S_{In} is the thermal neutron sensitivity of the fission chamber and is constant for a given fission chamber. Therefore, the output current $\bar{I}_n$ of the fission chamber is directly proportional to the mean thermal neutron flux at the place where the fission chamber is located. For absolute measurement (measurements for which every fission should be detected), atleast one fission fragment from each fission produced a recorded pulse. To achieve this, the thickness of the U-235 coating is limited so that fission fragments being produced anywhere in the layer of the uranium generate a pulse larger than that of alphas, betas, or gammas, which are always present.

An AD-DA converting board (Fig. 3.2) is inserted in the microcomputer control of the NIRR-1 as a channel for the computer to communicate with the outside. Various data of the reactor are collected to the computer by this interface board, and the reactor is controlled by the control signal sent by the computer, through the DA converter of this board. The ionization current of neutrons is sent to an automatic micro-current amplifier. The ionization current is converted by the amplifier into voltages V_1 and V_2 suitable for the AD interface board, and sent into No.0 and No.1 channels of the AD interface board

respectively. V_1 represents the significant digit of neutron ionization current, and V_2 represents the order of magnitude of the neutron ionization current. The gain of the automatic micro-current amplifier increases or decreases by times of 10, with its selection being fully automatic. When output voltage V_1 is higher than 4.7V, the range of the amplifier will be automatically changed to a higher one, whereas when V_1 is lower than 0.43V, the amplifier will automatically change over to the next lower range, thus ensuring that the neutron flux will have relatively high measuring precision within the whole measuring range (10^{-10}A ~ 5×10^{-4} A corresponding to 10^7 ~10^{13} n/cm^{2}s). In order to avoid the data acquisition from being carried out just at the moment of range changing, synchronous pulses are periodically produced by the computer through the DA converter. The range changing cannot take place until the synchronous pulse is received by the amplifier, and the next acquisition has a time-interval of ~80ms to the synchronous pulse, at this time, the amplifier has reached the stable status.

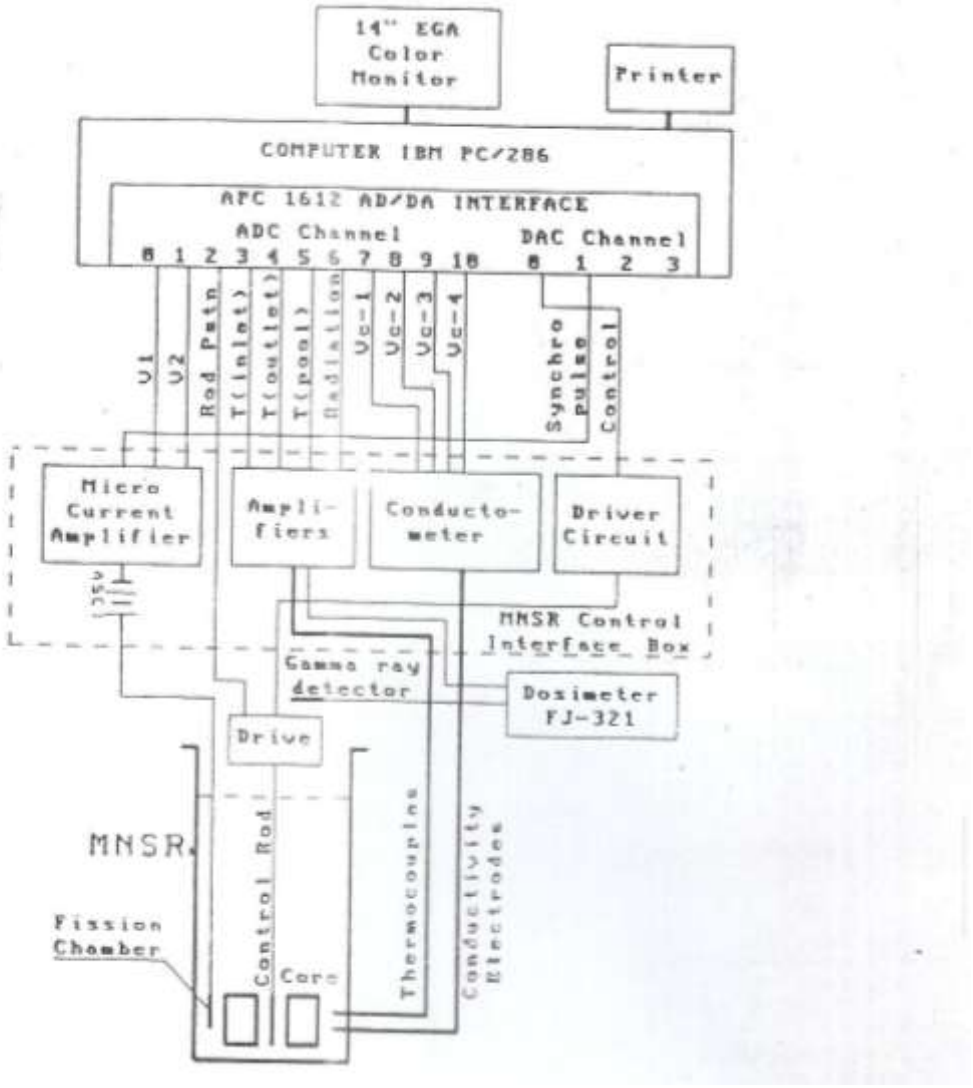

Fig. 3.2: Configuration of the microcomputer closed-loop control system for the MNSR (Liyu, 1992)

3.2.2 Temperature measurement

The measurement of the temperature difference between core outlet and inlet were accomplished with two alumel-chromel thermocouples. These two thermocouples are placed separately close to the core inlet orifice outside the side annulus beryllium reflector to measure the inlet temperature and close to the core outlet orifice at the upper part of the side annulus beryllium reflector to measure the outlet temperature. Combined, these two pairs of thermocouples monitored the temperature difference of the reactor coolant. The locations of the thermocouples are shown in Fig. 3.1.

The probe consist of two wire legs made from different metals (Nickel-Alumel/Nickel-Chromium) whose cold ends are compensated by the copper-constantan bridge. The wire legs are welded together to form one junction at the probe tip. When the detector is exposed to a temperature field, the resistance of the alumel-chromel wire varies with temperature. The bridge circuit in the balancing recorder is out of balance due to the variation of the resistance value, therefore a direct current electromotance is produced at the junction. These signals (inlet and outlet temperatures), having been amplified by 1000 times in the interface cabinet, are sent into No.3 and No.4 channels of the AD interface board (Fig. 3.2).

3.2.3 Gamma dose rate measurement

The experimental arrangement for gamma dose-rate measurement consisted of a Geiger-Muller counter detector. The detector (Model: FJ-321CG5 transistor 4–channel γ monitor, Precision: ±10%), which has a range of 0 - 999 μSv/hr is mounted on top cover plate of the reactor vessel near the surface of the pool and at the central position as shown in Fig. 3.3.

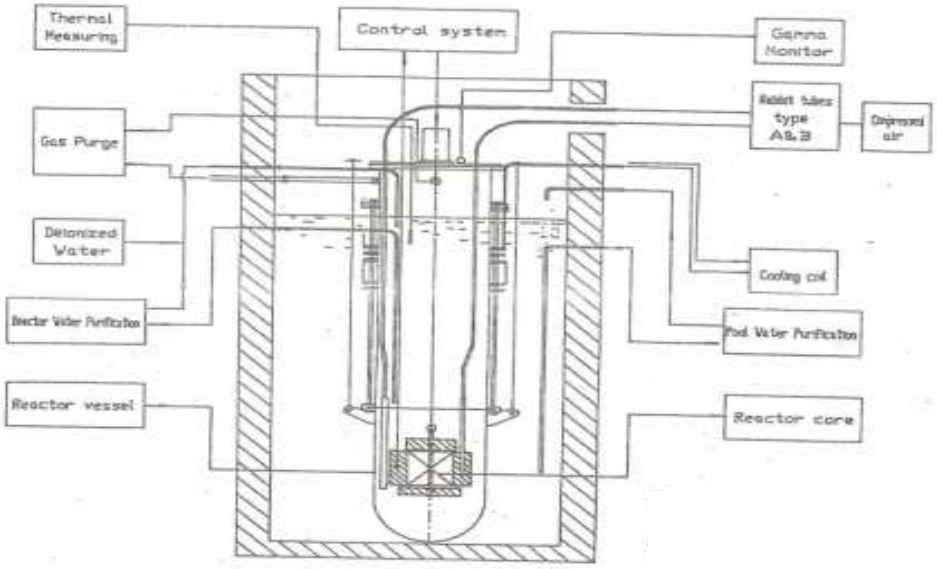

Fig. 3.3: MNSR Reactor and its System (Yongchun *et al.*, 1992)

The detector is a halogen counter that operate by utilizing the ionization produced by radiation as it passes through a gas. It consists of two electrodes to which a certain electrical potential is applied. The space between the electrodes is filled with a halogen gas. Ionizing radiation, passing through the space between the electrodes, dissipates part or all of its energy by generating electron-ion pairs. Both electrons and ions are charge carriers that move under the influence of the electrical field. Their motion induces a current on the electrodes, which through the electronics of the counter, is transformed in to a pulse, in which case particles are counted individually. The electric field inside the counter is so strong that a single electron-ion pair generated in the chamber is enough to initiate an avalanche of electron-ion pairs. This avalanche produced a strong signal with shape and height independent of the primary ionization and the type of particle, a signal that depends only on the electronics of the counter. The dose signal measured by the detector, after converted by FJ321 γ warning instrument, is sent to the interface cabinet in which it is amplified by 100 times, and then sent to No.6 channel of the AD interface board (Fig. 3.2).

Measurements of the neutron flux, dose-rate, core inlet and outlet temperatures were made at three stages:

a. The first one was immediately after the reactor start-up (0 minute), i.e., once the pre-determined power level of the reactor was reached and became stable. During this stage measurement, dose-rate measurements were made soon after the neutron flux reaches the value of 2×10^{11}, 5×10^{11}, and 10^{12} n/cm²-s at steady state conditions
b. The second one was at 105 minutes elapsed time of the reactor operation. At the second stage, the flux was lower to 2×10^{11} n/cm²-s and measurement for the dose-rate was made at various values for the thermal neutron flux but at steady state too.

c. The final one was made for five hours of reactor operation at half power, i.e., maximum neutron flux of 5×10^{11} n/cm²-s. In this final stage, dose-rate measurements for five hours of reactor operation was made.

d. For each of the above mentioned times, measurements were also made of the neutron flux, core inlet and outlet temperatures.

The above measured parameters are tabulated in chapter four and were then analyzed using SPSS.

3.3 USING SPSS FOR LINEAR REGRESSION ANALYSIS

The IBM SPSS Statistics 21 is a comprehensive system for analyzing data. SPSS Statistics can take data from almost any type of file and use them to generate tabulated reports, charts, and plots of distributions and trends, descriptive statistics, and complex statistical analyses. SPSS Statistics makes statistical analysis more accessible for the beginner and more convenient for the experienced user. Simple menus and dialog box selections make it possible to perform complex analyses without typing a single line of command syntax. The Data Editor offers a simple and efficient spreadsheet-like facility for entering data and browsing the working data file

Opening the SPSS for the first time will produce a dialog box which is not of any particular use, select *Don't show this dialog in the future*, and click on the *Cancel* button. This activates a window called data editor (Fig. 3.4). This is the main data editor window where all the data is entered, much like an Excel spreadsheet.

At the bottom of the data editor there are two tabs-Data view and Variable view. In Variable view (Fig. 3.5), we provide information about the values of the variables entered. In Data view (Fig. 3.6), the data editor works pretty much in the same manner as an Excel

spreadsheet. One can enter values in different cells, modify them and even cut and paste to and from an Excel spreadsheet.

The obtained data values shown in Tables 4.1, 4.2, and 4.3 were entered in to the data view of the data editor and the variables were labeled as Y and X, where Y defined the dependent variable and X defined the independent variable.

SPSS has 11 main menus on the top of data editor which provide access to every tool of the SPSS program. Click on the menu *Analyze*, which is a function that lets us perform all the statistical analysis. This will produce a drop down menu, choose *Regression* from that and click on *Linear* as shown in Fig. 3.7. The resulting dialog box is shown in Fig. 3.8.

Transfer the dependent variable in to the right-hand side box labeled *Dependent* and transfer the independent variable in to the box labeled *Independent*(s) by using the arrow buttons. Next, we click on *Statistics*, this will produce a dialog box labeled *Linear Regression: Statistics* as shown in Fig. 3.9. We then tick against the statistics we want in the output. The *Estimates* option gives the estimate of regression coefficients. The *Model fit* option gives the fit indices for the overall model. This two were selected in our case. Click on the *Continue* button to return to the main dialog box. Click on *Ok* in the main dialog box (Fig. 3.8) to run the analysis. The output result of the analyses at 0 minute and 105 minutes of the reactor operations are shown in chapter four.

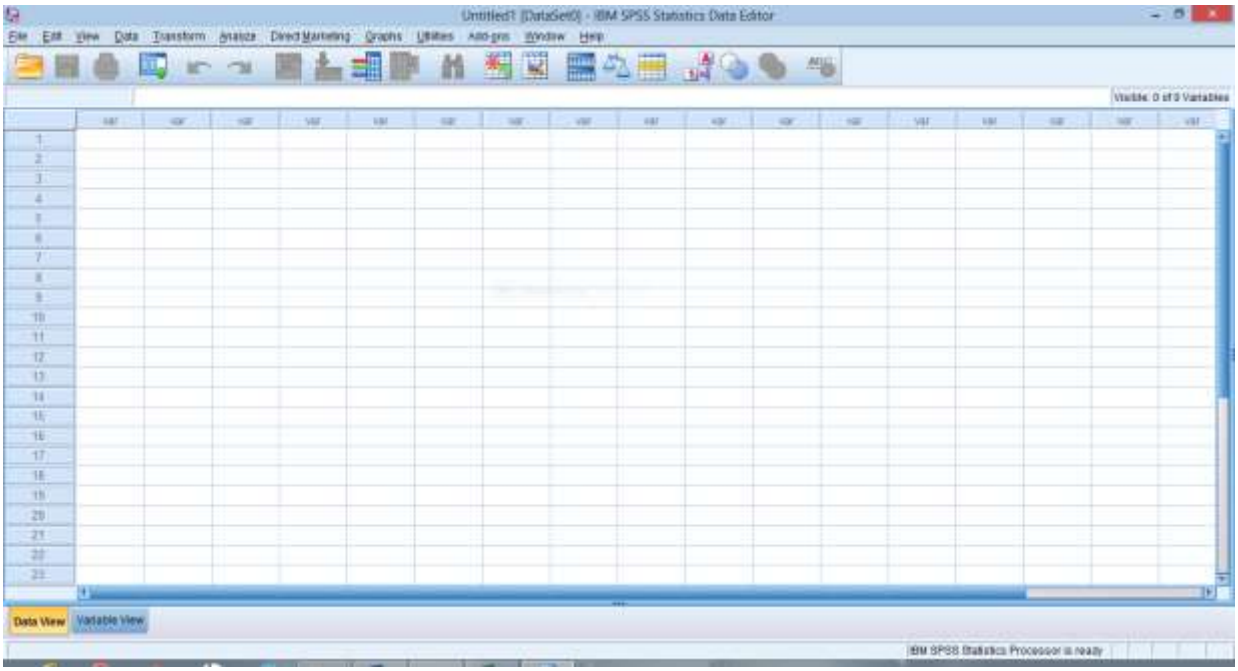

Fig. 3.4: Data editor dialogue box

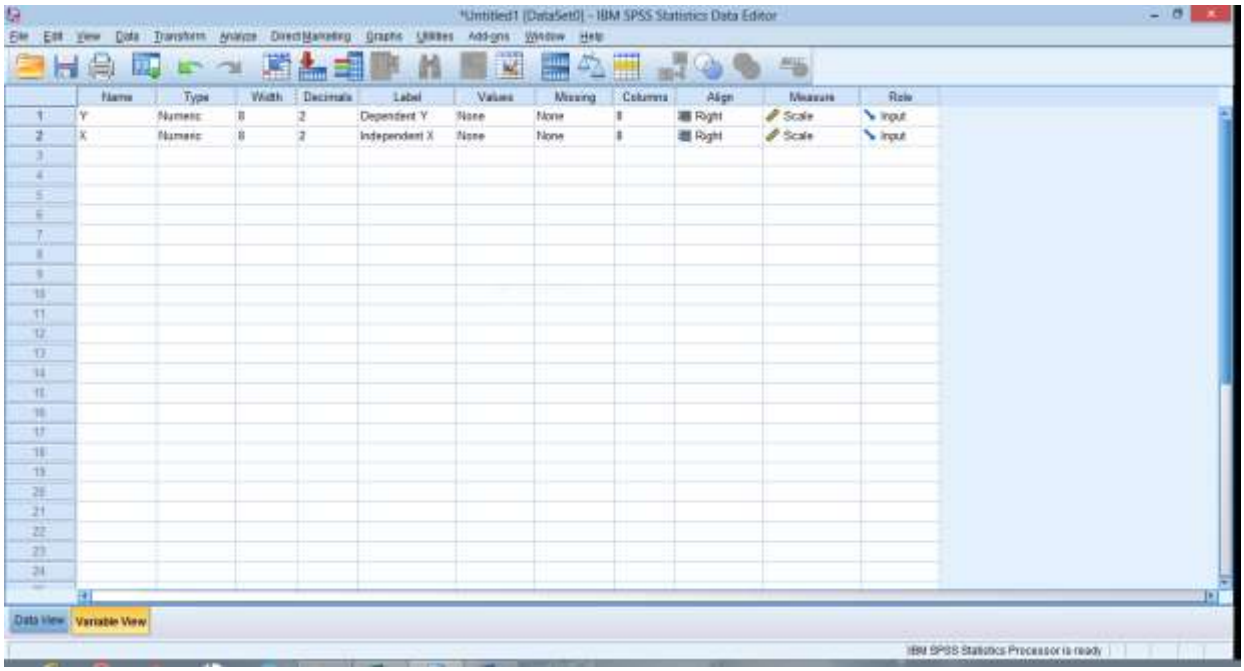

Fig. 3.5: Variable view dialogue box

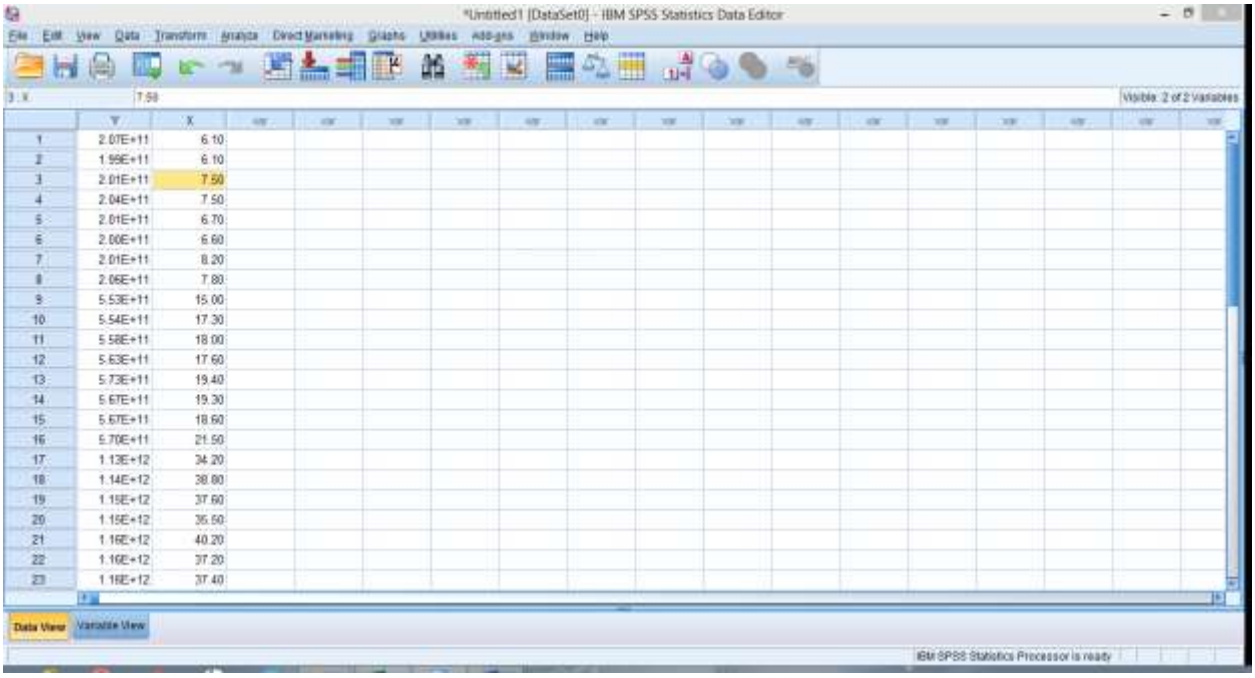

Fig. 3.6: Data view dialogue box

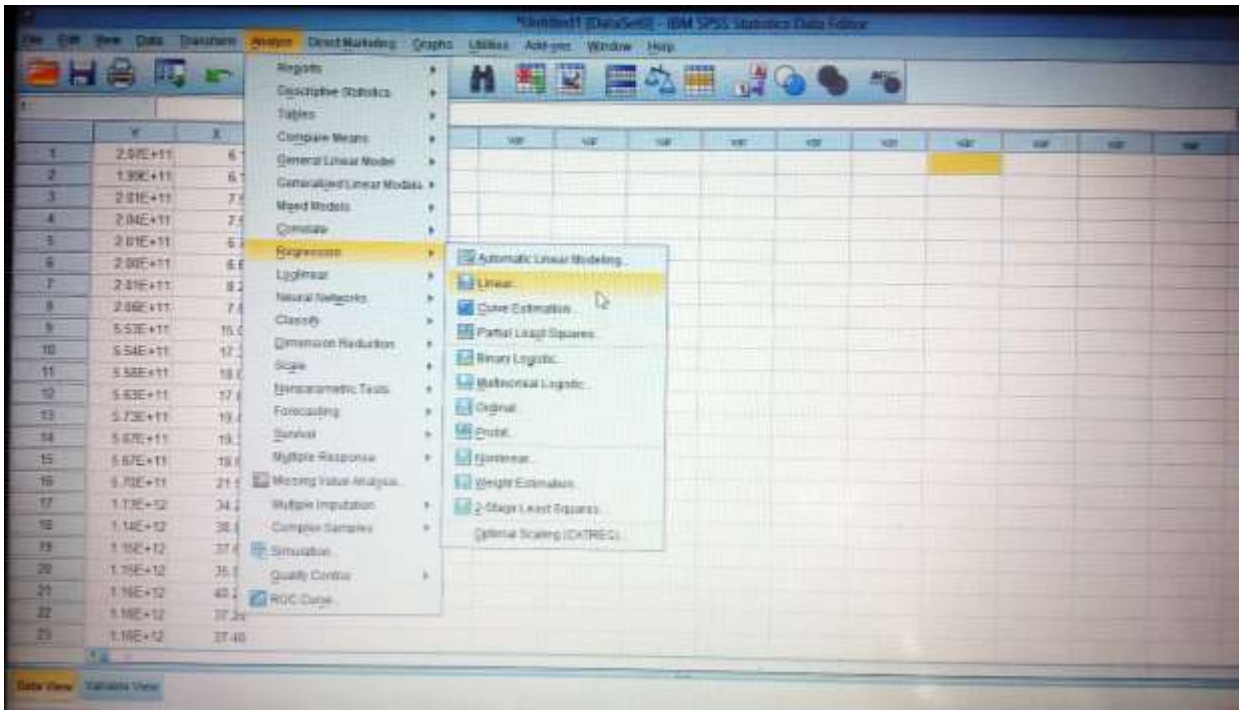

Fig. 3.7: Analyze > Regression > Linear dialogue box

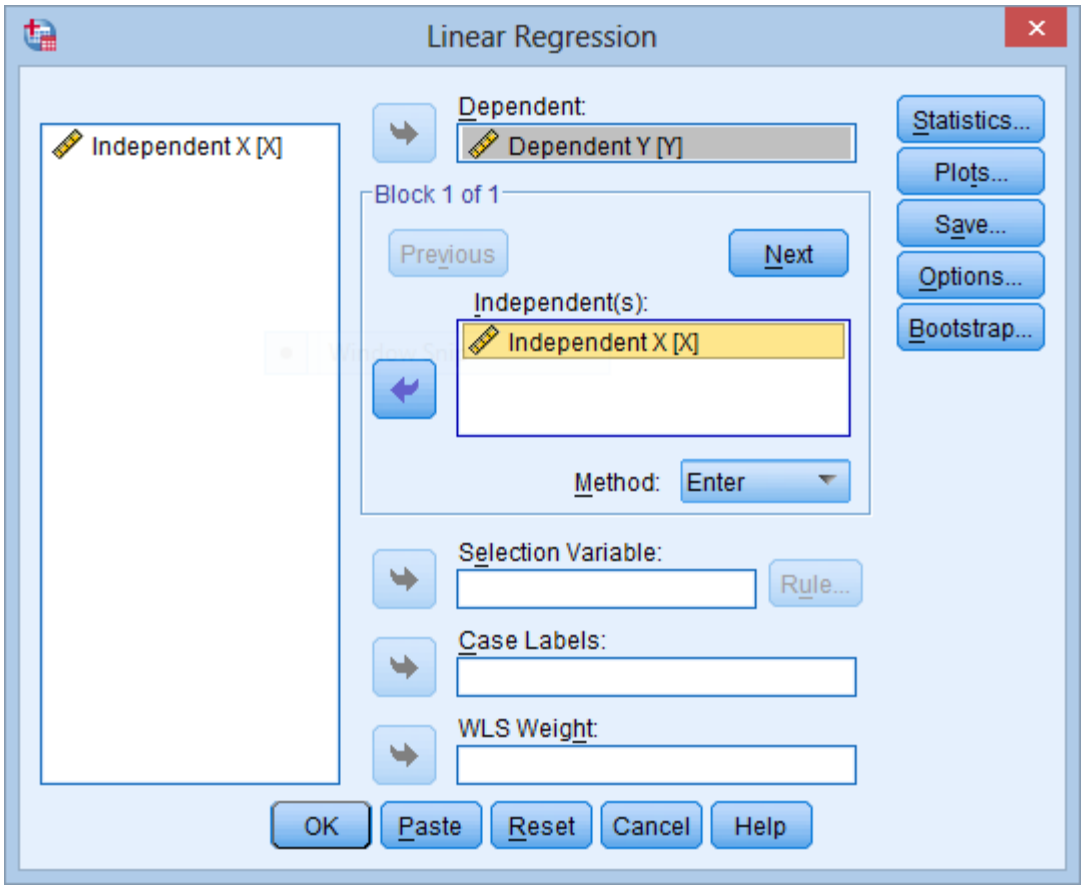

Fig. 3.8: Linear Regression dialogue box

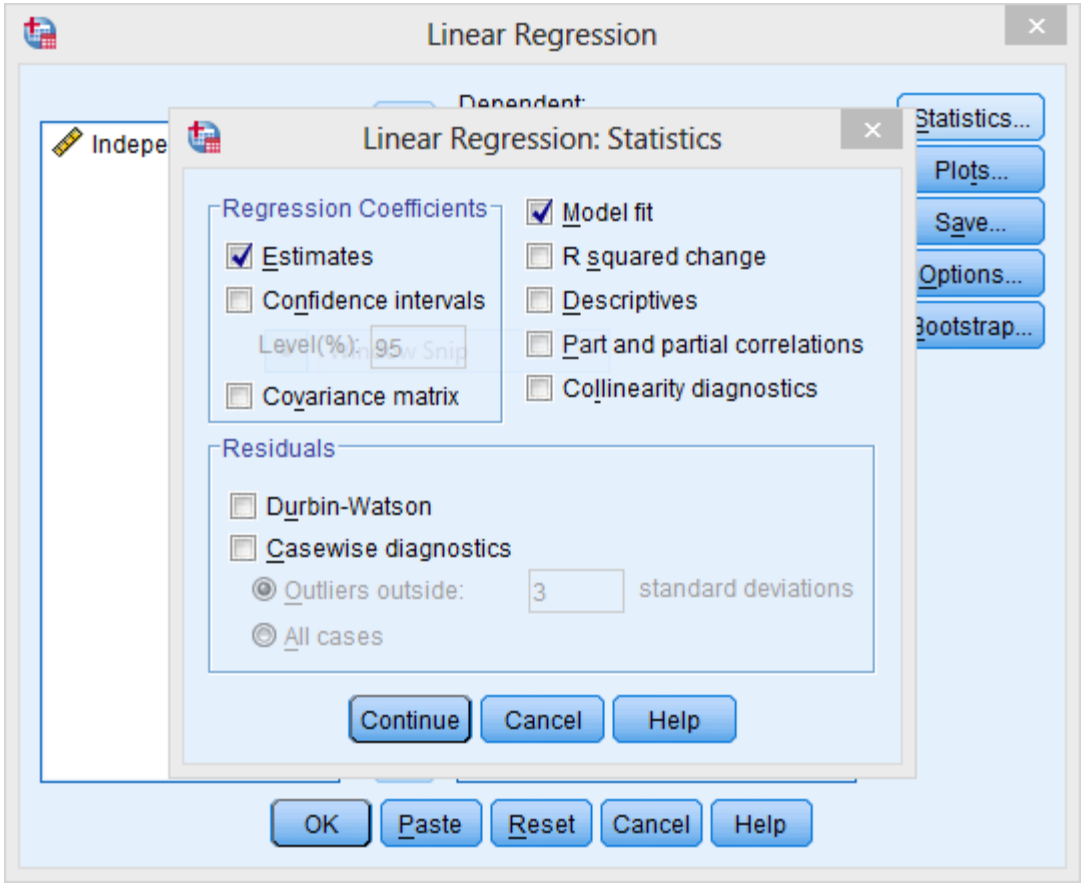

Fig. 3.9: Linear Regression: Statistics dialogue box

3.4 DATA EVALUATION

A SPSS was used for the linear regression analysis over the whole reactor operating range using the data obtained in Tables 4.1, 4.2 and 4.3, in order to evaluate the neutron flux and coolant temperature rise as a function of dose-rate.

The output result for the regression coefficients was used to construct the following Ordinary Least Squares (OLS) equations:

$$\phi = a_1 + b_1 \cdot \gamma \quad (3.1)$$

$$\Delta T = a_2 + b_2 \cdot \gamma \quad (3.2)$$

Where ϕ is the thermal neutron flux representing dependent variable (Y), γ is the dose-rate in µSv/h representing independent variable (X), a_1 and a_2 are constants, b_1 and b_2 are regression coefficients for the independent variables.

a. The reactor power as a function of dose-rate was obtained given by the equation:

$$P = 3.0 \times 10^{-8} (a_1 + b_1 \cdot \gamma) \quad (3.3)$$

Where P is the thermal power in watt.

b. The reactor power as a function of core inlet temperature and temperature difference was obtained through the equation (Ahmed *et al*., 2008)

$$P = \text{Exp}\left[Ln\left(\frac{\Delta T}{7.04 T_{in}^{-0.35}}\right)(0.59 + 0.0019 T_{in})^{-1}\right] \quad (3.4)$$

Where ΔT = Temperature difference between inlet and outlet orifices (°C).

T_{in} = Inlet temperature (°C).

c. The reactor power as a function of neutron flux was obtained given by the equation (Ahmed *et al*., 2008)

$$P = 3.0 \times 10^{-8} \phi \quad (3.5)$$

d. The average core coolant temperature as a function of inlet and outlet temperatures, power and dose-rate were obtained given by the equations (Khamis and Jamal, 2006)

$$\overline{T_{core}} = T_{in} + \frac{\Delta T}{2} \quad 3.6$$

$$\overline{T_{core}} = T_{in} + \frac{7.04 T_{in}^{-0.35} P^{(0.59+0.0019 T_{in})}}{2} \quad 3.7$$

$$\overline{T_{core}} = T_{in} + \frac{a_2 + b_2 \cdot \gamma}{2} \quad 3.8$$

CHAPTER FOUR
RESULTS AND DISCUSSION

The experimental results obtained in this work are hereby presented in Tables 4.1, 4.2, 4.3 and 4.8. All measurements were done at a steady state of reactor operation at different power level corresponding to preset flux values of 2×10^{11} n/cm²-s (6.2 kW), 5×10^{11} n/cm²-s (15.5 kW) and $1x10^{12}$ n/cm^2-s (31 kW) in order to enable us to predict the power corresponding to the rated thermal power by the manufacturer and also to investigate NIRR-1 steady state operation.

A SPSS software was used for the linear regression analysis using the data obtained in Tables 4.1, 4.2 and 4.3, in order to evaluate the neutron flux and coolant temperature rise as a function of measured dose-rate to predict the reactor power and average core coolant temperature at 0 minute and at 105 minutes elapsed time of the reactor operation as shown in Tables 4.4 and 4.7. The reactor power was also obtained using the temperature measurements (as shown in Table 4.5). The data values obtained in Table 4.8 were then used to investigate NIRR-1 steady state for five hours of operation as shown in Fig. 4.5.

The suggested methodology to estimate the reactor power as a function of dose-rate, neutron flux and temperature measurements were visualized by two steps. The first one calls for the measurements of the available dose-rate on top surface of the reactor vessel at the core centerline, neutron flux at the inner irradiation site and temperature at the core inlet orifice outside the side annulus beryllium reflector and the core outlet orifice at the upper part of the side annulus beryllium reflector during the initial stage of the reactor startup, i.e. at time of 0 minute for various preset neutron flux values starting from 2×10^{11}, 5×10^{11}, and 10^{12} n/cm²-s. The second one calls for same measurements at time of 105 minutes and at same various preset neutron flux values.

4.1 REGULAR NIRR-1 AT LOW POWER OPERATION FOR 1 HOUR 45 MINUTES

Table 4.1: Neutron flux, Temperatures and Dose-rate obtained at low power of preset flux value 2×10^{11} n/cm^2-s (6.2 kW) (Operation for 1 hour 45 minutes)

Time (h)	Measured Flux (10^{11}n/cm^{2}s)	T_{in} (℃)	T_{outlet} (℃)	ΔT (℃)	γ dose-rate ($\mu Sv/hr$)
0.00	2.07	24.8	32.6	7.8	6.1
0.25	1.99	25.2	32.5	7.3	6.1
0.50	2.01	25.9	33.4	7.5	7.5
0.75	2.04	26.6	34.1	7.5	7.5
1.00	2.01	27.0	34.1	7.1	6.7
1.25	2.00	27.4	34.6	7.2	6.6
1.50	2.01	26.9	34.5	7.6	8.2
1.75	2.06	27.9	35.1	7.2	7.8

4.2 REGULAR NIRR-1 AT HALF POWER OPERATION FOR 1 HOUR 45 MINUTES

Table 4.2: Neutron flux, Temperatures and Dose-rate obtained at half power of preset flux value 5×10^{11} n/cm^2-s (15.5 kW) (Operation for 1 hour 45 minutes)

Time (h)	Measured Flux (10^{11}n/cm^{2}s)	T_{in} (℃)	T_{outlet} (℃)	ΔT (℃)	γ-dose-rate ($\mu Sv/hr$)
0.00	5.53	25.2	37.9	12.7	15.0
0.25	5.54	26.1	39.2	13.1	17.3
0.50	5.58	28.1	40.0	11.9	18.0
0.75	5.63	29.3	41.5	12.2	17.6
1.00	5.73	29.8	41.6	11.8	19.4
1.25	5.67	30.3	42.3	12.0	19.3
1.50	5.67	31.1	42.6	11.5	18.6
1.75	5.70	32.0	44.4	12.4	21.5

4.3 REGULAR NIRR-1 AT FULL POWER OPERATION FOR 1 HOUR 45 MINUTES

Table 4.3: Neutron flux, Temperatures and Dose-rate obtained at full power of preset flux value 1x10^{12} n/cm^2-s (31 kW) (Operation for 1 hour 45 minutes)

Time (h)	Measured Flux (10^{12}n/cm^{2}s)	T_{in} (℃)	T_{outlet} (℃)	ΔT (℃)	γ-dose-rate ($\mu Sv/hr$)
0.000	1.13	28.0	46.7	18.7	34.2
0.083	1.14	30.0	48.0	18.0	38.8
0.416	1.15	33.0	52.3	19.3	37.6
0.749	1.15	35.0	53.1	18.1	35.5
1.082	1.16	37.0	55.4	18.4	40.2
1.415	1.16	38.0	55.1	17.1	37.2
1.748	1.16	38.0	56.3	18.3	37.4

4.4 SPSS OUTPUT OF LINEAR REGRESSION ANALYSIS

The output produced has several tables titled *Variables Entered/Removed*, *Model Summary*, *ANOVA* and *Coefficients* as shown in Figures 4.1, 4.2, 4.3 and 4.4. The table titled *Variables Entered/Removed* tells us about the independent variables and the regression method used. Here we can see that the independent variables were entered simultaneously for the analysis as we selected the *Enter* method. The second table titled *Model Summary* gives us the R values for assessing the overall fit of the model. The next table titled *ANOVA* indicates that the regression model predicts the dependent variable significantly well. The regression row displays information about the variation accounted for by our model. The residual row displays information about the variation that is not accounted for by our model. The regression and residual sums of squares are of different sizes and confirm that about 99.6%, 98.75, 97.8% and 96.2% of the variation in dependent variable are explained by the model. The significance values of the F statistics are less than 0.05 (except for Fig. 4.3), which indicated that, overall, the regression model statistically significantly predicted the outcome variables (i.e., it is a good fit for the data). The last table titled *Coefficients* gives the regression coefficients and their significance. The unstandardized regression coefficients are used as coefficients of independent variables along with the constant terms to construct an Ordinary Least Squares (OLS) equation and also to predict the thermal neutron flux and coolant temperature rise (Dependent variables) from dose rates (Independent variables).

Regression

Variables Entered/Removed[a]

Model	Variables Entered	Variables Removed	Method
1	Independent X[b]	.	Enter

a. Dependent Variable: Dependent Y

b. All requested variables entered.

Model Summary

Model	R	R Square	Adjusted R Square	Std. Error of the Estimate
1	.998[a]	.996	.992	42865407472.21092

a. Predictors: (Constant), Independent X

ANOVA[a]

Model		Sum of Squares	Df	Mean Square	F	Sig.
1	Regression	43302055684224 1350000000.000	1	43302055684224 1350000000.000	235.665	.041[b]
	Residual	18374431577586 75500000.000	1	18374431577586 75500000.000		
	Total	43485800000000 0000000000.000	2			

a. Dependent Variable: Dependent Y

b. Predictors: (Constant), Independent X

Coefficients[a]

Model		Unstandardized Coefficients		Standardized Coefficients	T	Sig.
		B	Std. Error	Beta		
1	(Constant)	32754101142.663	46109470345.790		.710	.607
	Independent X	32400320010.344	2110580877.550	.998	15.351	.041

a. Dependent Variable: Dependent Y

Fig. 4.1: Output of linear regression analysis of neutron flux versus dose-rate at time, t = 0 minute

Regression

Variables Entered/Removed[a]

Model	Variables Entered	Variables Removed	Method
1	Independent X[b]	.	Enter

a. Dependent Variable: Dependent Y

b. All requested variables entered.

Model Summary

Model	R	R Square	Adjusted R Square	Std. Error of the Estimate
1	.994[a]	.987	.987	45216520497.02271

a. Predictors: (Constant), Independent X

ANOVA[a]

Model		Sum of Squares	Df	Mean Square	F	Sig.
1	Regression	3345453226539597300000000.000	1	3345453226539597300000000.000	1636.292	.000[b]
	Residual	42935208243011170000000.000	21	2044533725857674700000.000		
	Total	3388388434782608600000000.000	22			

a. Dependent Variable: Dependent Y

b. Predictors: (Constant), Independent X

Coefficients[a]

Model		Unstandardized Coefficients		Standardized Coefficients	T	Sig.
		B	Std. Error	Beta		
1	(Constant)	-7445933649.929	18072954578.515		-.412	.685
	Independent X	30909839418.118	764128516.016	.994	40.451	.000

a. Dependent Variable: Dependent Y

Fig. 4.2: Output of linear regression analysis of neutron flux versus dose-rate at time, t = 105 minutes

Regression

Variables Entered/Removed[a]

Model	Variables Entered	Variables Removed	Method
1	Independent X[b]	.	Enter

a. Dependent Variable: Dependent Y

b. All requested variables entered.

Model Summary

Model	R	R Square	Adjusted R Square	Std. Error of the Estimate
1	.989[a]	.978	.955	1.15642

a. Predictors: (Constant), Independent X

ANOVA[a]

Model		Sum of Squares	Df	Mean Square	F	Sig.
1	Regression	58.269	1	58.269	43.572	.096[b]
	Residual	1.337	1	1.337		
	Total	59.607	2			

a. Dependent Variable: Dependent Y

b. Predictors: (Constant), Independent X

Coefficients[a]

Model		Unstandardized Coefficients		Standardized Coefficients	T	Sig.
		B	Std. Error	Beta		
1	(Constant)	6.138	1.244		4.935	.127
	Independent X	.376	.057	.989	6.601	.096

a. Dependent Variable: Dependent Y

Fig. 4.3: Output of linear regression analysis of coolant temperature rise versus dose-rate at time, t = 0 minute

Regression

Variables Entered/Removed[a]

Model	Variables Entered	Variables Removed	Method
1	Independent X[b]	.	Enter

a. Dependent Variable: Dependent Y

b. All requested variables entered.

Model Summary

Model	R	R Square	Adjusted R Square	Std. Error of the Estimate
1	.981[a]	.962	.961	.89329

a. Predictors: (Constant), Independent X

ANOVA[a]

Model		Sum of Squares	Df	Mean Square	F	Sig.
1	Regression	429.882	1	429.882	538.724	.000[b]
	Residual	16.757	21	.798		
	Total	446.639	22			

a. Dependent Variable: Dependent Y

b. Predictors: (Constant), Independent X

Coefficients[a]

Model		Unstandardized Coefficients		Standardized Coefficients	T	Sig.
		B	Std. Error	Beta		
1	(Constant)	5.308	.357		14.867	.000
	Independent X	.350	.015	.981	23.210	.000

a. Dependent Variable: Dependent Y

Fig. 4.4: Output of linear regression analysis of coolant temperature rise versus dose-rate at time, t = 105 minutes

4.4.1 R VALUES

R value (correction factor) represents the correlation between the observed values and the predicted value (based on the regression equation obtained) of the dependent variable. R Square is the square of R and gives the proportion of variance in the dependent variable accounted for by the set of independent variables chosen for the model. R Square is used to find out how well the independent variables are able to predict the dependent variables. However, the R Square value tends to be a bit inflated when the number of independent variables is more or when the number of cases is large. The adjusted R Square takes into account these things and gives more accurate information about the fitness of the model. The adjusted R Square values in our case (Figures 4.1, 4.2, 4.3 and 4.4) are 0.992, 0.987, 0.955 and 0.961 respectively. This tells us that the independent variables in our model account for 99.2%, 98.7%, 95.5% and 96.1% variance in the dependent variables. The R Square obtained in this work for the linear regression analysis of neutron flux versus dose-rate (Fig. 4.2) at 105 minutes of reactor operation was used for the reactor power predicted using dose-rate at 105 minutes of reactor operation.

4.5 REACTOR POWER AND DOSE-RATE

In order to evaluate the reactor power as a function of dose-rate, the linear correlation between neutron flux and dose-rate given by equation (3.1) was used for the linear regression analysis over the whole reactor operating range (using results obtained in Tables 4.1, 4.2 and 4.3).

Where the constant terms and the regression coefficients ($a_1$and b_1) have the values:

For t = 0 minute: a_1= 3.3×10^{10}, b_1 = 3.2×10^{10}

For t = 105 minutes: a_1= -0.74×10^{10}, b_1 = 3.1×10^{10}

Substituting the above constant terms and the regression coefficients into equation (3.3), the reactor power equation was then obtained in the form:

P = 0.3 (3.3 +3.2 · γ) for t = 0 minute

P = 0.27 (-0.74+3.1 · γ) for t = 105 minutes with Correction Factor 4.1

Where γ is the measured dose-rate in μSv/h and power is measured in kW.

The values of the dose-rate obtained at 0 minute for operation at 6.2 kW, 15.5 kW and 31 kW power levels are 6.1 $\mu Sv/h$, 15.0 $\mu Sv/h$ and 34.2 $\mu Sv/h$ respectively, the corresponding predicted power at this time were 6.8 kW, 15.4 kW and 33.8 kW respectively. The values of the dose-rate obtained at 105 minutes for operation at 6.2kW, 15.5 kW and 31 kW power levels were 7.8 $\mu Sv/h$, 21.5 $\mu Sv/h$ and 37.4 $\mu Sv/h$ respectively, the corresponding predicted power were 6.3 kW, 17.8 kW and 31.1 kW respectively.

Comparing the real data with values obtained using the above stated correlation (Eq. 4.1) for the power level as a function of dose-rate (as presented in Table 4.4, i.e., for various preset flux values during the initial startup and after 105 minutes of reactor operation reveals good agreement. Though, for the power level predicted after 105 minutes as a function of the measured dose-rate, a correction factor was introduced, as it slightly overestimate the real power. Such overestimation could be due to increase in gamma-rays as fission (isotopic composition) increases within 105 minutes time period, or due to the rise of the coolant temperature just above the core. The gamma-rays attenuation may be

reduce due to this effects, hence, increase the measured dose-rates. The rated power by the manufacturer and the results obtained during the initial startup of the reactor are in fair agreement, hence, no correction factor was introduced. As can be seen in Table 4.4, raw data were calculated using equation (3.3).

The results obtained at full power (31 kW) in this work tallies with the 29.5 kW calculated from fitting formula based on the stimulation test data during initial startup as reported in the NIRR-1 Safety Analysis Report (SAR, 2005). The results obtained at half and full power (15.5 kW and 31 kW) is also in good agreement with the (15.0 kW and 30.3 kW) and (13.7 kW and 28.8 kW) predicted at 0 and 90 minutes by Khamis and Jamal (2006) using the Syrian Miniature Neutron Source Reactor, and compare well with the rated thermal power by the manufacturer as can be observed in Table 4.4.

Table 4.4: Reactor power obtained using measured neutron flux and dose-rate at 0 and 105 minutes at preset flux values of 2×10^{11}, 5×10^{11} and 10^{12} n/cm²-s

Measured Flux (n/cm^2s)		Measured power from Eq. 3.5 (kW)		Measured dose-rate ($\mu Sv/hr$)		Reactor power from Eq. 4.1 (kW)				Rated thermal power(kW)
							At 105min			
At 0min	At 105min	At 0min	At 105min	At 0min	At 105min	At 0min	Raw	Corr	C.F	
$2.07x10^{11}$	$2.06x10^{11}$	6.21	6.18	6.1	7.8	6.8	7.0	6.3	0.9	6.2
$5.53x10^{11}$	$5.70x10^{11}$	16.60	17.10	15.0	21.5	15.4	19.8	17.8		15.5
$1.13x10^{12}$	$1.16x10^{12}$	33.90	34.80	34.2	37.4	33.8	34.6	31.1		31.0

Raw = Reactor power obtained without the Correction Factor (C.F) using dose-rate at 105 minutes of reactor operation.

Corr = Reactor power obtained with the Correction Factor (C.F) using dose-rate at 105 minutes of reactor operation.

4.6 REACTOR POWER AND TEMPERATURE

The semi-empirical relation between the core inlet temperature, coolant temperature rise and power level given in equation (3.4) was used for the power level predicted as a function of temperature measurements.

The results obtained for various preset neutron flux values during the initial startup (0 minute) and after 105 minutes of reactor operation are presented in Table 4.5. The values of the coolant temperature rise obtained (at 6.2 kW, 15.5 kW and 31 kW) during the first stage measurement (0 minute), i.e., once the pre-determined power-level of the reactor was reached and became stable were 7.8 °C, 12.7 °C and 18.7 °C and the corresponding predicted power were 6.9 kW, 14.8 kW and 28.0 kW. For the second stage, i.e., after 105 minutes elapsed time of the reactor operation, the values of the coolant temperature rise for the three power levels (6.2 kW, 15.5 kW and 31 kW) were 7.2 °C, 12.4 °C and 18.3 °C and the corresponding predicted power were 6.4 kW, 15.4 kW and 29.0 kW respectively. The results obtained at full power (31 kW) in this work compare well with 29.5 kW calculated from fitting formula based on the stimulation test data during initial startup as reported in the Nigeria Research Reactor -1 Safety Analysis Report (SAR, 2005). The results obtained in this work also compare well with 16.91 kW and 31.32 kW obtained (at half and full power respectively) by Ahmed *et al.,* 2008, and in good agreement with the rated thermal power by the manufacturer.

Table 4.5: Reactor power obtained using temperature measurements at 0 and 105 minutes

Preset Flux(n/cm^2s)	T_{in} (°C)		T_{out} (°C)		ΔT (°C)		Power from Eq.3.4 (kW)		Rated power(kW)
	At 0min	At 105min	At 0min	At 105min	At 0min	At 105min	At 0min	At 105min	
$2x10^{11}$	24.8	27.9	32.6	35.1	7.8	7.2	6.9	6.4	6.2
$5x10^{11}$	25.2	32.0	37.9	44.4	12.7	12.4	14.8	15.4	15.5
$1x10^{12}$	28.0	38.0	46.7	56.3	18.7	18.3	28.0	29.0	31.0

4.7 REACTOR POWER AND NEUTRON FLUX

In addition to the methods of determining the reactor power via the dose-rate and temperature measurements, the measured thermal neutron flux values were also used to predict the fission power of the reactor. In order to predict the core power using neutronic parameters, the linear relationship between the reactor power and neutron flux given in equation (3.5) was employed.

For the measured thermal neutron flux ($2.07x10^{11}$ n/cm^2-s, $5.53x10^{11}$ n/cm^2-s and $1.13x10^{12}$ n/cm^2-s at 0 minute, the predicted power as shown in Table 4.4 were 6.21 kW, 16.60 kW and 33.90 kW. The result obtained after 105 minutes elapsed time of the reactor operation for the measured thermal neutron flux were $2.06x10^{11}$ n/cm^2-s, $5.70x10^{11}$ n/cm^2-s and $1.16x10^{12}$ n/cm^2-s and the corresponding predicted power were 6.18 kW, 17.10 kW and 34.80 kW respectively. The results obtained at full power (31 kW) in this work is in good agreements with the 29.5 kW calculated from fitting formula based on the stimulation test data during initial startup as reported in the NIRR-1 Safety Analysis Report (SAR, 2005), 16.91 kW and 31.32 kW obtained (at half and full power respectively) by Ahmed *et al.*, 2008, and rated thermal power by the manufacturer.

Table 4.6: Comparison between reactor powers obtained using measured neutron flux, dose-rate and temperature at 0 and 105 minutes at preset flux values of 2×10^{11} n/cm^2-s (6.2 kW), 5×10^{11} n/cm^2-s (15.5 kW) and 10^{12} n/cm^2-s (31 kW)

Reactor power from measured neutron flux (kW)		Reactor power from measured dose-rate (kW)		Reactor power from measured temperature (kW)		Rated thermal power (kW)
At 0 min	At 105 min	At 0 min	At 105 min	At 0 min	At 105 min	
6.21±0.2%	6.18±0.3%	6.8±9.7%	6.3±1.6%	6.9±11.3%	6.4±3.2%	6.2
16.60±7.1%	17.10±10.3%	15.4±0.6%	17.8±14.8%	14.8±4.5%	15.4±0.6%	15.5
33.90±9.4%	34.80±12.3%	33.8±9.0%	31.1±0.3%	28.0±9.7%	29.0±6.5%	31.0

4.8 AVERAGE CORE TEMPERATURE AND DOSE-RATE

The reactor average core temperature was determined via three techniques. The first was evaluated as a function of inlet and outlet temperatures (Eq. 3.6), the second was as a function of reactor power (Eq. 3.7) while the third was as a function of dose-rate (Eq. 3.8).

In order to evaluate the average core temperature as a function of dose-rate, SPSS was employed for linear regression analysis using various correlations for coolant temperature rise and dose-rate over the whole reactor operating range at different preset flux values (using Tables 4.1, 4.2 and 4.3).

The linear relationship between coolant temperature rise and dose-rate (Eq. 3.2) was used to obtain the constant term and the regression coefficient:

For t = 0 minute: a_2 = 6.138, b_2 = 0.376

For t = 105 minutes: a_2 = 5.308, b_2 = 0.350

From equation (3.8), the average core temperature was calculated by substituting the constant term and the regression coefficient given above. Calculated results using equations (3.6), (3.7) and (3.8) are presented in Table 4.7 for both times, i.e. at 0 and 105 minutes. The results obtained for average core temperature as a function of inlet and outlet temperatures, reactor power and dose-rate are all in good agreement as can be seen in Table 4.7. Also, the values of the average core temperatures obtained in this work agree with that obtained by Khamis and Jamal (2006) using the Syrian MNSR.

Table 4.7: Average core temperature obtained using Eqs. (3.6), (3.7), and (3.8) with dose-rate and temperatures at 0 and 105 minutes

Preset	γdose-rate	T_{in}		T_{out}		ΔT		$\overline{T}_{core}$ (°C)		$\overline{T}_{core}$ (°C)		$\overline{T}_{core}$ (°C)	
Flux	$(\mu Sv/hr)$	(°C)		(°C)		(°C)		Eq. 3.6		Eq. 3.7		Eq. 3.8	
(n/cm^{2}s)		0min	105min	0min	105min	0min	105min	0min	105min	0min	105min	0min	105min
2x10^{11}		6.1	7.8	24.8	27.9	32.6	35.1	7.8	7.2	28.7	31.5	28.7	31.5	29.0	31.9
5x10^{11}		15.0	21.5	25.2	32.0	37.9	44.4	12.7	12.4	31.6	38.2	31.5	38.2	31.1	38.4
1x10^{12}		34.2	37.4	28.0	38.0	46.7	56.3	18.7	18.3	37.4	47.2	37.4	47.2	37.5	47.2

4.9 AVERAGE CORE TEMPERATURE AND DOSE-RATE FOR FIVE HOURS OF REACTOR OPERATION

Table 4.8 present measurements of dose-rate, core inlet, core outlet and average core temperatures, as well as coolant temperature rise across the core for a reactor operation of 5 hours, and were then used to investigate NIRR-1 steady state operation.

The obtained relationship between the average core temperature and time of reactor operation is presented in Fig. 4.5. As can be observed in the Figure, the graph starts as a linear one, but as time passes, it levels to a quasi-saturation. This shows that some kind of balance was achieved between heat generated in the core and heat being lost due to cooling of the core and partially accumulated in the water of the reactor vessel. This, in combination with the limited MNSR excess reactivity that is less than 0.5$ is a safety feature guaranteed by in-build negative temperature coefficient of reactivity, (Ahmed, *et al.*, 2011) just in case the reactor is left unattended for so long. The temperature were observed to be fairly stable after three hours of reactor operation. The fair stability was observed for one hour of operation after which a real steady state was achieved for two hours (as also indicated in Table 4.8). It was observed that for the experiment (Table 4.8), the coolant temperature rise ΔT as well as the average core coolant temperature $\overline{T}_{core}$ recoded during reactor operation are fairly constant with time. The thermal limitation have a range of value from 11.0˚C to 12.7˚C and average core temperature ranges from 31.6˚C to 38.6˚C .This is in agreement with one of the limiting conditions for safe operation of the reactor, which does not permit boiling as well as avoid speeding up corrosion of the NIRR-1 fuel elements which are in the form of U-Al_4 alloy clad in aluminum.

Table 4.8: Dose-rate and temperatures at half power of preset flux value 5×10^{11} n/cm²-s for 5 hours of reactor operation

Time (h)	Measured dose-rate (μSv/h)	T_{in} (°C)	T_{out} (°C)	ΔT (°C)	$\overline{T}_{core}$ (°C)
0	15.0	25.2	37.9	12.7	31.6
1	19.4	29.8	41.6	11.8	35.7
2	17.7	31.9	42.9	11.0	37.4
3	19.9	32.2	44.0	11.8	38.1
4	20.5	32.6	44.5	11.9	38.6
5	21.0	32.8	44.4	11.6	38.6

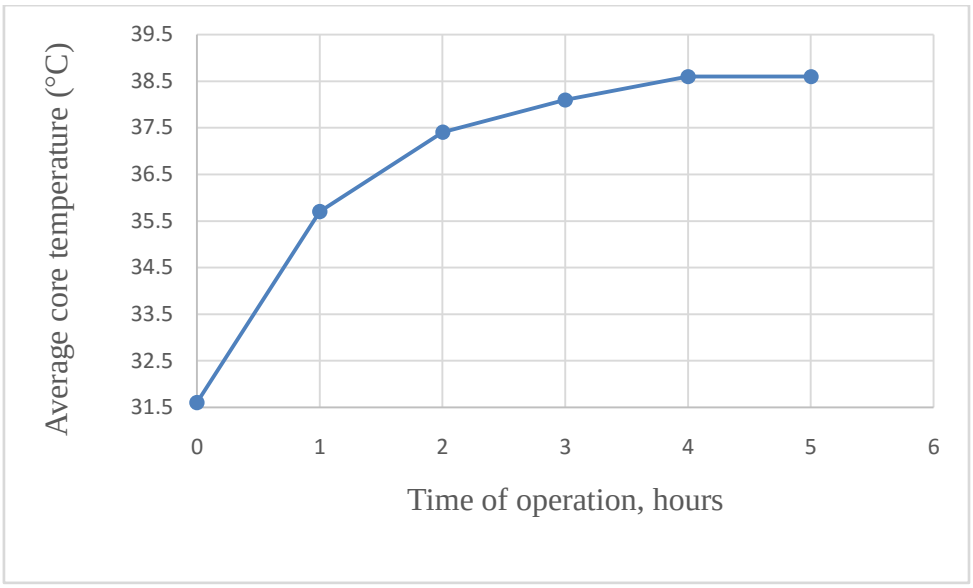

Fig. 4.5: A graph of average core temperature versus time of reactor operation at half power (15.5 kW)

CHAPTER FIVE
CONCLUSION AND RECOMMENDATION

5.1 CONCLUSION

In-core power prediction for NIRR-1 using measurements of dose-rate and temperature has been carried out. In this research, measurements of the dose rate, neutron flux, inlet and outlet temperatures were made and these measured parameters were explored to predict the core power. In order to cover the whole range of the reactor operation and give room for analyzing the accuracy of the different methods employed, the experiments were performed at three different power levels (6.2 kW (low power), 15.5 kW (half power) and 31 kW (full power)) and at three stages: The first one was immediately after the reactor start-up (0 minute). The second one was at 105 minutes elapsed time of the reactor operation. The final one was made at every hour for five hours of reactor operation at half power. The data obtained from the measurements were used to monitor the core power. The results obtained at 0 minute and 105 minutes using dose rate measurement at 6.2 kW, 15.5 kW and 31 kW were:(6.8 kW, 15.4 kW and 33.8 kW) and (6.3 kW, 17.8 kW and 31.1 kW) respectively. For temperature measurement, the results obtained at 0 minute and 105 minute were: (6.9 kW, 14.8 kW and 28.0 kW) and (6.4 kW, 15.4 kW and 29.0 kW) respectively. The results obtained at 0 minute and 105 minutes using measured neutron flux values were:(6.21 kW, 16.60 kW and 33.90 kW) and (6.18 kW, 17.10 kW and 34.80 kW) respectively. The results obtained at full power (31 kW) in this work compare well with 29.5 kW calculated from fitting formula based on the stimulation test data during initial startup as reported in the NIRR-1 Safety Analysis Report (SAR, 2005). The results obtained also compare well with the rated thermal power by the manufacturer. It was also

observed that the intensities of emitted gamma rays, temperatures and neutrons at any point in time at a preset power level from the reactor core are proportional to the reactor power. Comparing the results obtained using the stated parameters with the rated power by the manufacturer (Table 4.6), it was observed that the power obtained using does-rate is on average more accurate with deviations (9.7%, 0.6% and 9.0%) at 0 minute and (1.6%, 14.8% and 9.7%) at 105 minutes, and is therefore recommended for all users of MNSR as well as for routine estimation of NIRR-1 power. The values of the average core temperature obtained in this work is in good agreement with the values obtained by Khamis and Jamal 2006.

5.2 RECOMMENDATION

We recommend that:

1 The stability of the reactor power via temperature measurement be investigated at other power levels such as lower power and full power.

2 The adoption of dose-rate measurement for routine estimation of NIRR-1 power.

3 New source code be written for the microcomputer control of the reactor to accommodate the findings of this research work.

References

Ahmed, Y.A., Ewa, I.O.B., Umar, I.M., (2002). Effective resonance energy and non-ideality of epithermal neutron flux distribution in neutron activation analysis. Nigerian Journal of Physics 14 (1), 82–85.

Ahmed, Y.A., Ewa, I.O.B., Umar, I.M., (2006). Variations in nuclear data and its impact on INAA. Journal of Applied Science 6 (8), 1692–1697.

Ahmed, Y.A., Balogun, G.I., Jonah, S.A., Funtua, I.I., (2008). The Behavior of Reactor Power and Flux Resulting from Changes in Core-Coolant Temperature for a Miniature Neutron Source Reactor, Annals of Nuclear Energy Vol. 35: 2417-2419. Elsevier Science.

Ahmed, Y.A., Gabdo, H., (2008). Nuclear data in k_0-standardization method of neutron activation analysis. Bayero Journal of Physics and Mathematical Sciences 1 (2), 173–181.

Ahmed, Y.A., Mansir, I.B., Yusuf, I., Balogun, G.I., Jonah, S.A., (2011). Effects of core excess reactivity and coolant average temperature on maximum operable time of NIRR-1 miniature neutron source reactor. Nuclear Engineering and Design 241, 1559–1564.

Akaho, E.H.K., Anim-Sampong, S., Maakuu, B.T., Dadoo-Amoo, D.N.A., (2000). Dynamic feedback characteristics of Ghana research reactor-1. Journal of the Ghana Science Association 2 (3), 200–208.

Akaho, E.H.K., Nyako, B.J.B., (2002). Characterization of neutron flux spectra in irradiation channel of MNSR reactor, using the Westcott-formalism for the *k0* neutron activation analysis method, Applied Radiation and Isotopes, 57, 265-273.

Akaho, E.H.K., S. Anim-Sampong, D.N.A., Dodoo-Amoo, B.T., Maakuu, G., Emi Reynolds, E.K., Osae, H.O., Boadu, S.A., Bamford, (2003). Ghana Research Reactor-1 Final Safety Analysis Report. Ghana Atomic Energy Technical Report, GAEC-NNRIRT-90.

Alhassan, E., (2009). Analysis of reactivity temperature coefficient for light water moderated HEU-UAl4 and LEU-UO2 lattices of MNSR. M.Phil thesis, University of Ghana, Legon, Accra.

Arakani, M., Gharib, M., (2009). Reactor core power measurement using Cherenkov Radiation and its Application in Tehran Research Reactor.

Armozd, H.R., Gharib, M., Afarideh, H., Ghergherehchi, M., Niar, A.A., Jafarzadeh, M., (2011). Determination of Tehran research reactor power by ^{16}N gamma detection. Annals of Nuclear Energy, Vol. 38, pages 2667–2672.

Azande, S., Balogun, G.I., Ajuji, A.S., Jonah, S.A., Ahmed, Y.A., (2010). The use of WIMS and CITATION codes in fuel loading required for the conversion of HEU MNSR core to LEU. Annals of Nuclear Energy 37, pp. 1223–1228 (Elsevier Science).

Balogun, G.I., (2003). Automating some analysis and design calculations of miniature neutron source reactor at CERT (I). Annals of Nuclear Energy 30, 81–92.

Balogun, G.I., Jonah, S.A., Ahmed, Y.A., Sa'adu, N., (2004). Results of On-site Zero power and Criticality Experiments for the Nigeria Research Reactor-1. Internal Report CERT/NIRR-1/ZP/01, April.

Bebbs, E.H., Clay-Price Jr, H., (1958). Naval Research Laboratory-Research Reactors, Part-VIII Neutron Flux Measurements and Power Determination, NRL Report 5196, Washington, DC.

Beeley, P.A., Brushwood, J.M., Henesy, M.G., Collins, M.W., Haywood, C.A., (1997). Determination of in-core power in low energy research reactors by measurement of ^{16}N and ^{18}F in the primary coolant. J. Radioanal. Nucl. Chem. 215 (1), 135–139.

Bullock, J.B., (1965). Absolute Power Measurements of the Ford Nuclear Reactor. Paper Presented at the ANS Conference on Reactor Operating Experience at Jackson Lake Lodge, Wyoming; 0-1.

CNSC, (2003). Science and Reactor Fundamentals–Reactor Physics Technical Training.

Coulon, R., Normand S., Ban, G., Barat, E., Montagu, T., Dautremer, T., Brau, H.P., Dumarcher, V., Michel, M., Barbot, L., Domenech, T., Boudergui, K., Bourbotte, J.M., Jousset, P., Barouch, G., Ravaux, S., Carrel, F., Saurel, N., Frelin-Labalme, A.M., Hamrita, H., and Kondrasovs, V., (2011). Delayed gamma power measurement for sodium-cooled fast reactors. Nucl. Eng. Design 241 (1), pp. 339-348.

DOE, (1993). Fundamentals Handbook–Nuclear Physics and Reactor Theory. Vol. 1 and 2, Modules 1, 2, 3 and 4. Department of Energy, United States of America, Pages 5, 15, 48, 23-29.

Erradi, L., Santamarina, A., Litaize, O., (2003).The Reactivity Temperature Coefficient Analysis in Light Water Moderated UO2 and UO2-PuO2 Lattices. Nuclear Science and Engineering, 44:47-74.

Freedman, D.A., (2005). Statistical Models. Theory and Practice, Cambridge University Press.

Gaur, A.S., Gaur, S.S., (2009). Statistical Methods for Practice and Research. A guide to data analysis using SPSS, Second edition, 108-116.

Glasstone, S., Sesonske, A., (1994). Nuclear reactor engineering reactor design basics Vol. 1 and 2, Fourth ed., Springer, 0-412-98521-7 0-412-98531-4.

Guo, Z., (1983). Physical calculations for commercial MNSR. CIAE Technical Report.

Hainoun, A., Alisa, S., (2005). Full-scale modeling of the MNSR reactor to simulate normal operation, transients and reactivity insertion accidents under natural circulation conditions using the thermal hydraulic code ATHLET. Nuclear Engineering and Design 235, 33–52.

IAEA/AECL/ANL, (1995). Interregional Training Course on Safety in the Operation of Research Reactors, Lecture Notes.

Jalali, M., Abdi, R.M., Mostajaboddavati, M., (2013). Reactor Power Measurement by Gamma and Neutron Radiation in Heavy Water Zero Power Reactor. Annals of Nuclear Energy 57, pages 368–374.

Jonah, S.A., Balogun, G.I., Umar, I.M., Mayaki, M.C., (2005). Neutron Spectrum Parameters in Irradiation Channels of the Nigeria Research Reactor-1 (NIRR-1) for the k0-NAA Standardization. Journal of Radioanalytical and Nuclear Chemistry 266 (1), 83–88.

Jonah, S.A., Umar, I.M., Oladipo, M.O.A., Balogun, G.I., Adeyemo, D.J., (2006). Standardization of NIRR-1 irradiation and counting facilities for instrumental neutron activation analysis. Applied Radiation and Isotopes 64, 818–822.

Jonah, S.A., Liaw, J.R., Matos, J.E., (2007). Monte Carlo simulation of core physics parameters of the Nigeria Research Reactor-1(NIRR-1). Annals of Nuclear Energy 54, 953-957.

Khamis, I., Jamal, M.J., (2006). Prediction of the in-core Power and the average core temperature using dose-rate measurements in the Syrian Miniature Neutron Source Reactor. Journal of Radioanalytical and Nuclear Chemistry 269 (1), 81–85.

Klimov, Y.V., Koperkin, V.I., Mikaelyan, L.A., Ozerov, K.V., Siner, V.V., (1994). Neutrino method remote measurement of reactor power and power output. Atomic Energy 76 (2), 123-127.

Knoll, G.E., (2000). Radiation detection and measurement, 3rd edition, ISBN 0-471-07338, John Wiley & Son.

Krull, W., (2000). Research Reactors Under Threat. Nucl. Eng. Intl.

Kutner, M.H., Nachtsheim, C.J., Neter, J., (2004). Applied Linear Regression Models, 4th edition, McGraw-Hill/Irwin, Boston, 25.

Landau, S., Everitt, B.S., (2004). A Handbook of Statistical Analyses Using SPSS. A CRC Press Company, London, 38-43.

Lamarsh, J. R., (1966). Introduction to Nuclear Reactor Theory, Addison-Wesley Publishing Company, 4120, Reading, Massachusetts, USA.

Lamarsh, J.R., Baratta, J.A., (1982). Introduction to Nuclear Engineering, Third Edition. Prentice Hall Upper Saddle River, New Jersey.

Lamarsh, J. R., Baratta, A. J., (2001). Introduction to Nuclear Engineering, Prentice Hall.

Letter to the editor, (1970). Absolute measurement of reactor power by neutron noise analysis. J. Nucl. Energy 24, 525–526.

Lhuillier, D., (2009). Reactor neutrino monitoring. Nucl. Phys. B 188, 112–114 (Proc. Suppl.).

Lilley, J., (2001). Nuclear Physics Principles and Applications, pp. 1-393, 0-471-97936-8.

Liyu, W., (1992). The Micro Computer Closed-loop Control System for MNSR. China Institute of Atomic Energy, MNSR training material, pg. 2-8.

Lu, Y., (1964). Measurement of reactor power level by a Nitrogen-16 monitor. Thesis in Nuclear Engineering. The Pennsyvania State University. The Graduate School, Department of Nuclear Engineering.

Manca, P., (2011). Calculations to Support Absolute Thermal Power Calibration of the Slovenian TRIGA Mark II Reactor. 20th International Conference. Nuclear Energy for New Europe 2011 /Bovec/ Slovenia/September 12-15.

Mesquita, A.Z., Rezende, H.C., Prado Souza, R.M.G., (2011). Thermal power calibrations of the IPR-R1 TRIGA reactor by the calorimetric and the heat balance methods. Prog. Nucl. Energy 53, 1197–1203.

Mirza, S.M., (1996). Simulation of over-power transient in Tank-in-pool type research reactors. Annals of Nuclear Energy, 24(24): 871-881.

Mogil'ner, A.I., Shvetsov, D.M., (1967). Statistical methods of measuring the absolute power of a reactor. J. Nucl. Energy 21, 87–95.

Musa, M.A., Funtua, I.I., Mallam, S.P., Arabi, A.S., (2011). Determination of Absorbe and Effective Dose from Natural Background Radiation around a Nuclear Research Facility. American Journal of Environmental Sciences 7 (2): 173-177.

Musa, Y., Ahmed, Y.A., Yamusa, Y.A., Ewa, I.O.B., (2012). Determination of Radial and Axial Neutron Flux distribution in irradiation channel of NIRR-1 using foil activation technique. Annals of Nucl. Energy 50(2012) 50–55.

Ott, K.O., Bezella, A.W., (1989). Introductory Nuclear Reactor Statics. Revised Edn. American Nuclear Society, Illinois. ISBN: 0-894-48033-2.

Parry, S.J., (1991). Activation Spectrometry in Chemical Analysis, John Wiley and Sons, New York.

Ravishankar, N., Dey, D.K., (2002). A First Course in Linear Model Theory, Chapman and Hall/CRC, Boca Raton, 101.

Sadeghhi, N., (2010). Estimation of reactor power using N-16 production rate and its radiation risk assessment in Tehran Research Reactor (TRR). Nucl. Eng. Des. 240, 3607–3610.

SAR, (2005). Final Safety Analysis Report of Nigeria Research Reactor-1. CERT Technical Report-CERT/NIRR-1/FSAR-01.

Schaeffer, N.M., (1973). Reactor Shielding for Nuclear Engineers. US Atomic Energy Commission Office of Information, TID-25951, 12–59.

Scott, A.J., (2012). Illusions in Regression Analysis. International Journal of Forecasting (Forthcoming) 28 (3): 689.

Shi, S., (1990). Low Power Research Reactor Thermal Hydraulics; IAEA Workshop on Low Power Research Reactors. CIAE, Beijing.

Shi, Y.Q., Li, Y.G., (2001). Measurement of fast fission factor for Heavy Water Zero Power Reactor (HWZPR) by solid state nuclear track detector. Radiat. Meas. 34,605–607.

Soulfanidis, N., (1983). Measurement and Detection of Radiation. Taylor and Francis, Washington, DC.

Straka, M., (1984). Power Calibration Using the Thermal Expansion of Pool Water, UMRR/851, Rolla, USA.

Sturm, D., (1961). Reactor Laboratory Experiments, ANL-641, USA.

Whittemore, W.J., Razvi, J., Shoptaugh Jr, J.R., (1988). Power Calibrations for TRIGA™ Reactors, General Atomics, GEN-39, San Diego, California, USA.

Tsypin, S.G., Lysenko, V.V., Musorin, A.I., Bogachek, L.N., Bai, V.F., Kuz'min, V., Koshelev, A.B., (2003). N-16 ray diagnostics of a nuclear reactor in a nuclear power plant. Atomic Energy 95 (3), 609–612.

Yamamoto, T., Miyoshi, Y., (1999). Improvement of neutron source introduction method for absolute measurements of low reactor power. J. Nucl. Sci. Technol. 36, 1069-1075.

Yang, Y., (1992). Reactor complex manual. CIAE Technical Report, Code MNSR-DC-3.

Yongchun, G., Jijin, G., Huabai, T., Yuewen, Y., (1992). Miniature Neutron Source Reactor (MNSR) general descriptions. MNSR document, China Institute of Atomic Energy. Code: MNSR-DC-1, pg. 28.

Zhang, Y., (1984). Simulated heat transfer test for MNSR, CIAE Technical Report.

Zhou, Y., 1985. IAEA-TECDOC-384 "Technology and Use of Low Power Research Reactors". Report of IAEA Consultants Meeting, Beijing, China 30 April – 3 May, pg. 8998.

Zhu, G., (1990). Neutron Physics Experiments on Low Power Research Reactor, IAEA Workshop on Low Power Research Reactors, CIAE Beijing, China.